Available online at www.sciencedirect.com

ScienceDirect

Geochimica et Cosmochimica Acta 213 (2017) 216–236

Geochimica et Cosmochimica Acta

www.elsevier.com/locate/gca

Hydrogen isotope fractionation in leaf waxes in the Alaskan Arctic tundra

William C. Daniels[a,b,*], James M. Russell[a], Anne E. Giblin[b], Jeffrey M. Welker[c], Eric S. Klein[c], Yongsong Huang[a,*]

[a] Brown University, Department of Earth, Environment, and Planetary Sciences, 324 Brook St., Providence, RI 02906, United States
[b] Marine Biological Laboratory, The Ecosystems Center, 7 MBL St., Woods Hole, MA 02543, United States
[c] University of Alaska-Anchorage, Department of Biological Sciences, 3211 Providence Dr., Anchorage, AK 99508, United States

Received 24 August 2016; accepted in revised form 17 June 2017; Available online 23 June 2017

Abstract

Leaf wax hydrogen isotopes (δD_{wax}) are increasingly utilized in terrestrial paleoclimate research. Applications of this proxy must be grounded by studies of the modern controls on δD_{wax}, including the ecophysiological controls on isotope fractionation at both the plant and landscape scales. Several calibration studies suggest a considerably smaller apparent fractionation between source water and waxes (ε_{app}) at high latitudes relative to temperate or tropical locations, with major implications for paleoclimatic interpretations of sedimentary δD_{wax}. Here we investigate apparent fractionation in the Arctic by tracing the isotopic composition of leaf waxes from production in modern plants to deposition in lake sediments using isotopic observations of precipitation, soil and plant waters, living leaf waxes, and waxes in sediment traps in the Brooks Range foothills of northern Alaska. We also analyze a lake surface sediment transect to compare present-day vegetation assemblages to ε_{app} at the watershed scale. Source water and ε_{app} were determined for live specimens of *Eriophorum vaginatum* (cottongrass) and *Betula nana* (dwarf birch), two dominant tundra plants in the Brooks Range foothills. The δD of these plants' xylem water closely tracks that of surface soil water, and reflects a summer-biased precipitation source. Leaf water is enriched by 23 ± 15‰ relative to xylem water for *E. vaginatum* and by 41 ± 19‰ for *B. nana.* Evapotranspiration modeling indicates that this leaf water enrichment is consistent with the evaporative enrichment expected under the climate conditions of northern Alaska, and that 24-h photosynthesis does not cause excessive leaf water isotope enrichment. The ε_{app} determined for our study species average −89 ± 14‰ and −106 ± 16‰ for *B. nana n*-alkanes and *n*-acids, respectively, and −182 ± 10‰ and −154 ± 26‰ for *E. vaginatum n*-alkanes and *n*-acids, which are similar to the ε_{app} of related species in temperate and tropical regions, indicating that apparent fractionation is similar in Arctic relative to other regions, and there is no reduced fractionation in the Arctic. Sediment trap data suggest that waxes are primarily transported into lakes from local (watershed-scale) sources by overland flow during the spring freshet, and so δD_{wax} within lakes depends on watershed-scale differences in water isotope compositions and in plant ecophysiology. As such, the large difference between our study species suggests that the relative abundance of graminoids and shrubs is potentially an important control on δD_{wax} in lake sediments. These inferences are supported by δD_{wax} data from surface sediments of 24 lakes where ε_{app}, relative to δD_{xylem}, averages −128 ± 13‰ and

* Corresponding authors at: Brown University, Department of Earth, Environment, and Planetary Sciences, 324 Brook St., Providence, RI 02906, United States (W.C. Daniels).

E-mail addresses: william_daniels@brown.edu (W.C. Daniels), james_russell@brown.edu (J.M. Russell), agiblin@mbl.edu (A.E. Giblin), jmwelker@uaa.alaska.edu (J.M. Welker), esklein@uaa.alaska.edu (E.S. Klein), yongsong_huang@brown.edu (Y. Huang).

http://dx.doi.org/10.1016/j.gca.2017.06.028

−130 ± 8‰ for *n*-acids and *n*-alkanes, respectively, and co-varies with vegetation type across watersheds. These new determinations of plant source water seasonality and ε_{app} for the Arctic will improve the δD_{wax} paleoclimate proxy at high latitudes.

Keywords: Leaf waxes; Water isotopes; Biomarkers; Precipitation; Isotope fractionation; Arctic; Tundra; Sediment

1. INTRODUCTION

Hydrogen and oxygen isotope ratios in meteoric water (δD and $\delta^{18}O$) are well-established tracers of environmental processes (Dansgaard, 1964; Ehleringer and Dawson, 1992; Vachon et al., 2010; Welker, 2012). When preserved in the geologic record, these isotopes serve as robust tools for paleoclimate reconstructions (Feakins et al., 2012; Jasechko et al., 2015; Klein et al., 2016; Konecky et al., 2016). Hydrogen isotope ratios of plant leaf waxes are an increasingly utilized proxy because they are abundant in many sediments (Huang et al., 2004; Sachse et al., 2004), are stable over long time periods (Yang and Huang, 2003), and their isotopic composition (δD_{wax}) primarily reflects the δD of precipitation ($\delta D_{precipitation}$) (Sternberg, 1988; Sauer et al., 2001; Huang et al., 2004; Sachse et al., 2004; Sachse et al., 2010). The δD_{wax} is depleted by a fractionation factor (ε_{app}) relative to $\delta D_{precipitation}$ due to several isotope-discriminating processes that occur between precipitation and leaf wax synthesis and deposition (Sessions et al., 1999; Chikaraishi et al., 2004; Sachse et al., 2012; Kahmen et al., 2013b). Accurate estimates of ε_{app} are therefore fundamentally important to guide climatic interpretations of ancient δD_{wax} (Polissar and Freeman, 2010; Yang et al., 2011; Garcin et al., 2012; Feakins, 2013; Niedermeyer et al., 2016), and ideally, to quantitatively determine $\delta D_{precipitation}$ and climate variations in geological time.

Numerous analyses of δD_{wax} from lake sediments and living plants in temperate and tropical regions have begun to converge on average ε_{app} values of −100 to −130‰ (Sauer et al., 2001; Sachse et al., 2004; Smith and Freeman, 2006; Hou et al., 2008; Garcin et al., 2012; Kahmen et al., 2013a; Liu et al., 2016), with *n*-alkanes displaying slightly greater isotope discrimination than *n*-alkanoic acids (Chikaraishi and Naraoka, 2007). Recent estimates of ε_{app} at high-latitude sites, however, are dramatically different. Shanahan et al. (2013) estimated ε_{app} of −61‰ for C_{26} and C_{28} alkanoic acids using lake surface sediment samples from Baffin Island in the High Arctic (latitude: 63–73 °N) compared against mean annual precipitation isotopes compositions for source water estimated from the Online Isotopes in Precipitation Calculator (OIPC) geospatial model (Bowen and Revenaugh, 2003). Porter et al. (2016) produced similar ε_{app} values for both long-chain *n*-acids and long-chain *n*-alkanes by comparing fossil waxes to adjacent fossil water (interpreted as mean annual precipitation formed simultaneously with the waxes) in loess sections in the Canadian sub-Arctic (latitude: 63.5 °N). Based on growth chamber experiments, these low ε_{app} values in high-latitude, continuous light environments have been suggested to result from plant stomata remaining open throughout the 24-hour sunlit period, thus driving high daily rates of evapotranspiration and high leaf water isotope enrichment (Yang et al., 2009).

In contrast, Wilkie et al. (2012) studied lake sediment waxes (*n*-acids) in northern Siberia (latitude: 67°N) and reported ε_{app} of −101‰ with respect to estimates of mean annual precipitation isotope composition, and ε_{app} of −110‰ with respect to the measured isotopic composition of spring streamflow. Sachse et al. (2004) report ε_{app} of −100 to −135‰ for long chain *n*-alkanes from Arctic Europe using similar methods. These contrasting results raise the following questions: (1) is ε_{app} latitude-dependent? (2) is ε_{app} highly variable across high latitude biomes? and (3) are observations of small ε_{app} an artifact of relying on estimated, rather than measured, source water isotope compositions?

The apparent fractionation of Arctic δD_{wax} is extremely important to understanding past and current polar climate change. δD_{wax} records in polar regions have been interpreted as both summer and mean annual temperature change on time-scales from the Holocene to the Paleocene (Pagani et al., 2006; Feakins et al., 2012; Thomas et al., 2012; Pautler et al., 2014; Porter et al., 2016), with implications for the Earth's equilibrium climate sensitivity and future response to rising greenhouse gases. For example, calculations of Paleocene/Eocene $\delta D_{precipitation}$ from ancient wax δD and an ε_{app} of −100‰ to −130‰ reveal extreme warmth and moisture convergence in the Arctic during the Paleocene/Eocene thermal maximum (PETM) (Pagani et al., 2006). If a smaller ε_{app} of −60‰ is used, however, the estimated $\delta D_{precipitation}$ during this time period was similar to modern $\delta D_{precipitation}$, and not strongly enriched, casting doubt on our understanding of Arctic climate during the PETM. Paleoclimate inferences for Antarctica during the mid-Miocene (Feakins et al., 2012) are likewise sensitive to whether an ε_{app} value of −100‰ or −60‰ is used to calculate $\delta D_{precipitation}$. Similarly, two temperature anomaly estimates for the last glacial maximum in western Canada (Pautler et al., 2014; Porter et al., 2016), which rely on the same δD_{wax} data but different values of ε_{app}, differ by 14 °C. Clearly, large deviations of ε_{app}, caused either by inaccurate assessment of plant source water δD values, by enhanced leaf water isotope enrichment during 24-h transpiration, or by large changes in vegetation assemblages, would complicate interpretations of polar δD_{wax}.

With the exception of the study by Wilkie et al. (2012), investigations of ε_{app} in the Arctic have thus far relied on estimated $\delta D_{precipitation}$ values from the OIPC model (Bowen and Revenaugh, 2003; Yang et al., 2011; Shanahan et al., 2013) or measurements of relict (frozen) water in permafrost (Porter et al., 2016). Both of these methods could be insufficient for determining ε_{app} considering the complexity of precipitation seasonality, soil water dynamics, and plant water use dynamics (Alstad et al., 1999; Welker et al., 2005; Young et al., 2017). Moreover, previous efforts to quantify the effects of 24-h photosynthesis in greenhouse experiments used plants that do not currently grow in the Arctic, such as *Metasequoia* (redwood), and the hypothesized increase in leaf water isotopic values due to greater transpiration was not accompanied by leaf water isotopic measurements (Yang et al., 2009). Direct measurements of plant xylem and leaf waters in Arctic field conditions would provide a more robust estimate of plant source water isotope values (Welker, 2000; Leffler and Welker, 2013). To our knowledge, no previous study has traced Arctic D/H fractionation from precipitation to leaf wax production in living plant tissues, changes in δD_{wax} through the growing season, nor variations in δD_{wax} associated with native Arctic vegetation, ecosystem integration, and sedimentation.

Three ecophysiological controls are particularly important to estimating ε_{app}. First, the seasonal fluctuations in $\delta D_{precipitation}$ relative to the timing of wax synthesis by plants can lead to differences in source water isotope composition for different regions or plant types (Alstad et al., 1999; Vachon et al., 2010). Accurate determination of seasonal changes in plant source water is especially important in the Arctic, where $\delta D_{precipitation}$ can change drastically through the year. Secondly, although the δD of xylem water (δD_{xylem}) generally reflects $\delta D_{precipitation}$ (White et al., 1985), the δD of leaf water (δD_{leaf}) is sensitive to factors that govern leaf water evaporation including relative humidity (Kahmen et al., 2013a; Tipple et al., 2015), species effects (leaf morphology, canopy height, water use efficiency) (Sullivan and Welker, 2007), and possibly day length (Yang et al., 2009). Again, quantifying enrichment in δD_{leaf} in the Arctic could test whether strong apparent fractionation results from 24-h photosynthesis. Third, biosynthetic fractionation during leaf wax generation varies by plant type. Eudicots are typically characterized by ε_{app} value of −156 to −85‰ while monocotyledons have a larger fractionation ranging from −190 to −120‰ (Hou et al., 2007; Gao et al., 2014a; Liu et al., 2016). Fractionation values of arctic plants tend to fall into these ranges (Wilkie et al., 2012; Thomas et al., 2016), although there is also support fractionation values as small as 60‰ at the plant-scale in the Arctic (Yang et al., 2011). Biosynthetic fractionation has generally been treated as a species-specific constant, but Newberry et al. (2015) indicate that biosynthetic fractionation varies seasonally because of the greater contribution of H atoms from stored carbohydrates during the period of leaf flush. Together, these effects may help explain the discrepancies in high-latitude estimates of ε_{app}, and also suggest that shifting vegetation communities can significantly alter values of ε_{app}.

The main objectives of this study are (1) to assess the importance of 24-h daylight on D/H fractionation by determining ε_{app} at the plant and landscape scales in the Arctic tundra, and (2) to describe the environmental controls, especially vegetation assemblages, on δD_{wax}. We report paired measurements of the δD of precipitation, soil water, xylem water, leaf water, and leaf waxes of two dominant plant taxa from the Alaskan Arctic that constrain the apparent fractionation in these Arctic plants. We use sediment trap data to assess changes in δD_{wax} through the growing season, and a regional survey of leaf waxes preserved in lake surface sediment to estimate ε_{app} and evaluate whether local vegetation variations explain between-lake variation in ε_{app}. Together, these results provide a comprehensive framework for interpreting δD_{wax} in the Arctic tundra and illustrate the utility of combining plant-level and ecosystem-level studies of D/H fractionation.

2. SITES, SAMPLES, AND METHODS

2.1. Site description

The study area is located in the northern foothills of the Brooks Range at the Toolik Lake Natural Research Area (68.5 °N, 149.5 °W; Fig. 1). Annual temperature averages −8.5 °C, while the summer (JJA) averages 9 °C. Monthly temperatures are above zero from mid-May to early-September. Precipitation averages 312 mm, with roughly 60% of precipitation occurring primarily as rain during summer months (JJA; Fig. 2) (Cherry et al., 2014). Summer relative humidity averages 75%. The soils are characterized by continuous permafrost with summer thaw depths ranging from 30 to 200 cm (Shaver et al., 2014). The growing season is characterized by an average date for first leaf appearance of June 3, with full spring green-up occurring in late-June and plant senescence occurring in late August and September (Toolik Environmental Data Center Team, 2016).

Glacier activity emanating from the Brooks Range was spatially and temporally variable through the late Pleistocene, giving rise to three landscape surfaces of varying age and vegetation in our study area (Fig. 1) (Walker and Walker, 1996; Hamilton, 2003). These consist of the Sagavanirktok (>125 ka), Itkillik I (~60 ka), and the Itkillik II (~25–11.5 ka) surfaces. The Sagavanirktok surface is gently sloping, has substantial organic soil accumulations, and contains few lakes. The most recently deglaciated terrain (Itkillik II) in contrast, has steeper slopes, shallow bedrock, and contains a higher density of lakes; the Itkillik I surface is intermediate with regards to geomorphology. Vegetation distributions across our study region are presented by Walker and Maier (2008), who identify nine major vegetation classes. Of these, moist acidic tundra (MAT) is the most prevalent and occurs on all landscapes (Fig. 1). MAT consists of tussock-sedges (*Eriophorum vaginatum*), non-tussock sedges (*Carex bigelowii*), mosses, and dwarf shrubs (primarily *Betula nana*). The younger glacial surfaces, being better drained, more poorly weathered, and having shallower organic soils, tend to contain greater areas of dry tundra complex and non-acidic tundra dominated by prostrate shrubs (*Salix arctic*, *S. reticulata*) with a general absence of mosses and sedges, although MAT can also be found on the younger surface. Salix and Betula complexes are commonly found along streams and in watertracks. In general, similar plant communities can be found around much of the Arctic (CAVM Team, 2003).

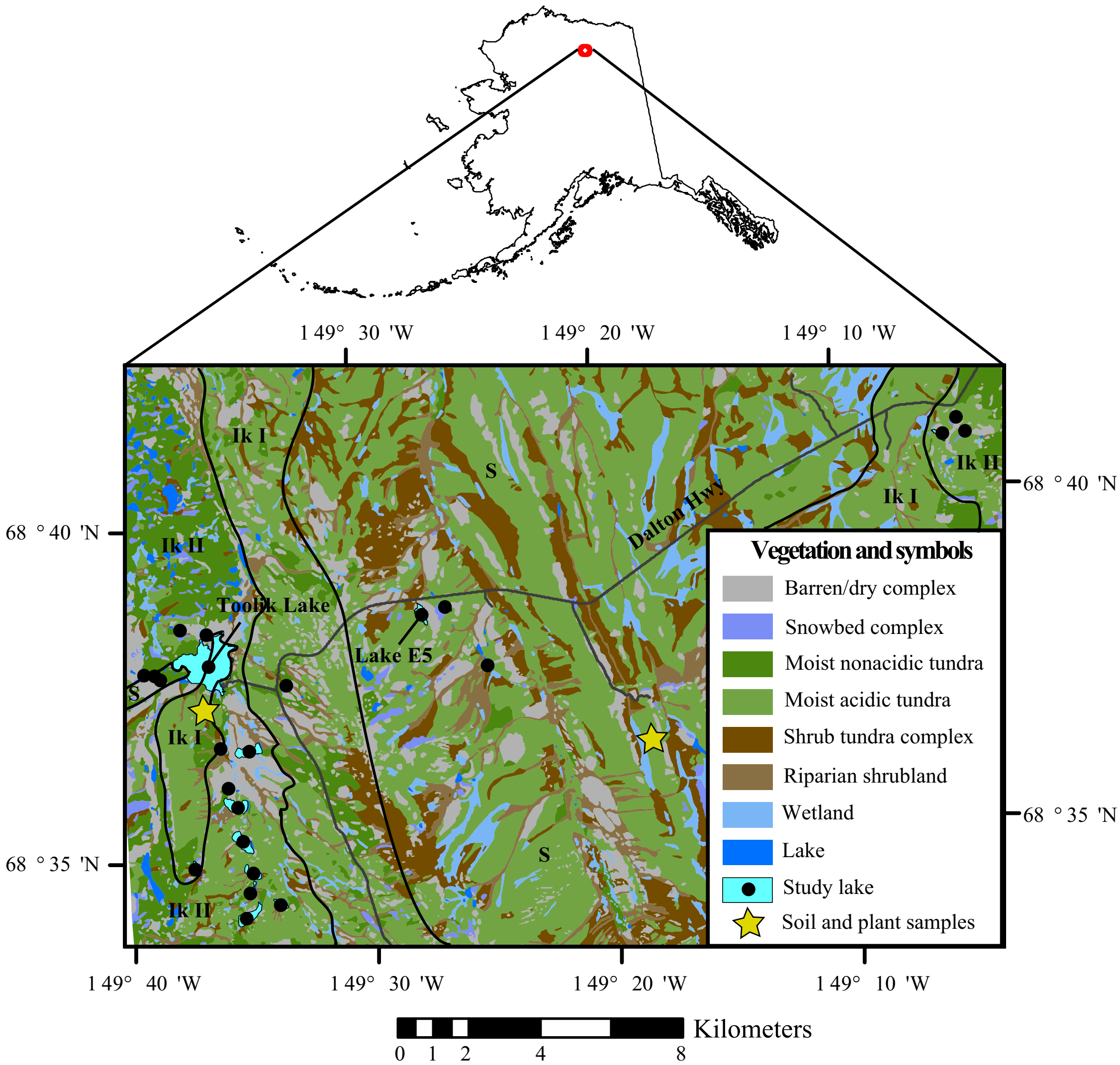

Fig. 1. Map of study lakes (black dots) and plant sampling locations (yellow stars). The basemap shows the diversity of plant communities in the study area and a generalization of the glacial ages referenced in the text (http://www.arcticatlas.org/). Sediment traps were deployed in Lake E5 and Toolik Lake, as labelled on the map. (For interpretation of the references to colour in this figure legend, the reader is referred to the web version of this article.)

2.2. Sample collection

2.2.1. Vegetation and water isotopes

Precipitation isotopes were collected on a year-round event basis from 1993 to present (Klein et al., 2016). Not all events were measured, but in total, the isotopic composition of 254 precipitation events were measured. We calculated an amount-weighted mean annual precipitation isotope signature using binned monthly values of $\delta D_{precipitation}$ and monthly values of precipitation amount (Toolik LTER Environmental Data Center).

Soil water and vegetation samples were collected on August 6, 2013, July 17/19, 2014, and August 7/8, 2014 between 10:00 and 16:00. Sampling sites were located within the Imnavait Creek watershed (68.61 °N, 149.30 °W) on the Sagavanirktok glacial surface and the Toolik Lake watershed (68.62 °N, 149.61 °W) on the Itkillik I glacial surface. Both sites are characterized as moist acidic tundra, the most prevalent vegetation community in the region. Soil water isotope profiles (δD_{soil}) were collected during each sampling. Soil water was collected to a depth of 92.5 cm using two methods. We used soil probes fit with a 50 mL syringe to extract water from the thawed organic horizon at 0, 5, 10, 15, and 20 cm soil depth. Water was pushed through a combusted GFF filter into plastic scintillation vials and frozen. Where soil was too dry or frozen to use this method we collected 5–10 cm^3 soil samples from pits to be melted or distilled. Permafrost soil samples were provided from soil pits dug by Collin Ward, Jason Dubkowski, and Katherine Harrold of the ARC LTER (Ward and Cory, 2015).

We measured the δD_{xylem}, $\delta D_{leaf\ water}$, and δD_{wax} for two tundra plants, *Eriophorum vaginatum* (cottongrass) and *Betula nana* (dwarf birch). These species are two of

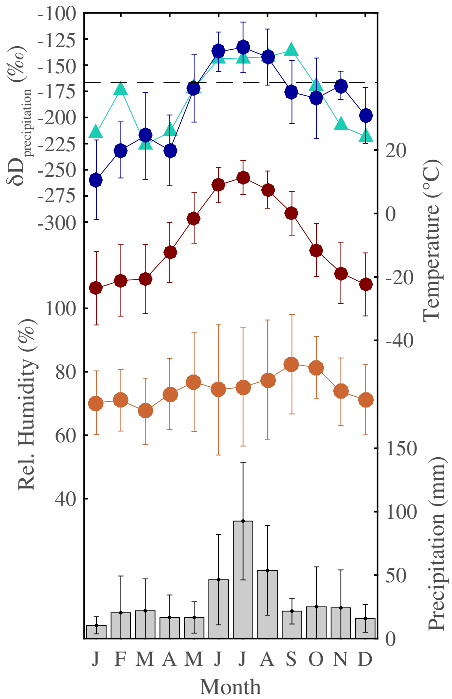

Fig. 2. Climatology and $\delta D_{precipitation}$ at Toolik Lake including monthly precipitation isotopes (blue – precipitation event measurements; teal – OIPC estimate; the horizontal dashed line is the weighted mean annual $\delta D_{precipitation}$ value of −166‰), air temperature (red), relative humidity (orange), and precipitation (gray bars). (For interpretation of the references to colour in this figure legend, the reader is referred to the web version of this article.) *Source:* Toolik Environmental Data Center; accessed Nov. 2016.

the most dominant species in the Arctic tundra (Walker et al., 1994; Chapin III et al., 1995) and serve as model species for monocots (*E. vaginatum*) and dicots (*B. nana*), which are two major plant groupings with respect to D/H fractionation (Gao et al., 2014a). From the same sites where soil water was collected, sets of roots, stems, and leaves from individual plants were collected. A total of 14 sets of *B. nana* and 9 sets of *E. vaginatum* samples were collected across all sampling efforts. Live roots were separated from aboveground components and immediately cleaned of clinging soil and soil water. For *B. nana*, several 5-cm segments of stem were cut from each plant and composited. Likewise, >20 *B. nana* leaves were collected and composited to ensure sufficient leaf water yield for isotopic analyses and to homogenize variability among leaves. For *E. vaginatum*, stems were not distinguished from leaves, and approximately 20 leaves were composited for each plant. All plant parts were stored frozen in Whirlpak™ bags until processing.

2.2.2. Sedimentary waxes

We analyzed δD_{wax} from surface sediment samples from 24 lakes near Toolik Field Station to compare to our ε_{app} values from individual plants and to assess the ecosystem-integrated values of ε_{app} (Fig. 1). Lakes were selected that are accessible by foot and that span the various glacial surfaces and vegetation types (Table 2). Surface sediments were collected from lake depocenters in 2011 and 2013 using a gravity corer, sectioned in the field, and kept frozen until analysis (Longo et al., 2016). We analyzed the surface 1.0 cm from all lakes, which based on ^{210}Pb-based accumulation rates from Toolik Lake (Cornwell and Kipphut, 1992), integrates approximately 10–25 years. To test if local (watershed-scale) differences in vegetation assemblages can affect the ε_{app} observed in lake sediments, we compared the ε_{app} with the relative abundance of major vegetation types within each lake's watershed using single and multiple linear regression. Vegetation distributions were derived from vegetation maps, which translate aerial photographs into nine discrete plant complexes, downloaded from the Alaska Geobotany Center (Walker and Maier, 2008) (Fig. 1, Table 2).

Sediments were also collected from sediment traps deployed in Toolik Lake and Lake E5 (ARC LTER). Sediment traps were deployed in May 2014 and collection vials were replaced 4 times during the summer giving 2–6 week resolution. Traps were deployed approximately 2 m above the lake floor.

2.3. Sample processing and analysis

2.3.1. Water isotopes

Water was extracted from plant tissues and bulk soils using cryogenic vacuum distillation (Gao et al., 2012). Soil and plant samples were heated under vacuum in extraction vials to 100 °C and the resulting vapor was collected in a vial in liquid nitrogen. Samples were immediately thawed and transferred into 4 mL vials, sealed with parafilm, and stored at 4 °C. For all soil water samples, 3 mg of activated charcoal (particle size <150 μm) was added to the samples to remove excessive dissolved organic matter. Samples reacted overnight and the charcoal was filtered using a GFF filter. Precipitation, soil water, and plant water samples were analyzed for $\delta^{18}O$ and δD on a Picarro L1102-i cavity ring-down spectrometer at Brown University. Samples were analyzed with Picarro ChemCorrect software to test for the effects of organic contaminants and no samples were flagged as problematic. The 1σ analytical error determined from replicate standards was 0.09‰ for $\delta^{18}O$ and 0.57‰ for δD.

2.3.2. Biomarker processing

Lipids were extracted from leaf residues after removing leaf water. Approximately 100 mg of leaf material was sonicated for 15 min in dichloromethane:methanol (1:1 v/v), with three solvent rinses. Lipids were extracted from freeze-dried surface sediments and sediment trap samples using a Dionex Accelerated Solvent Extractor (ASE) 350 with dichloromethane:methanol (9:1 v/v). Lipids were separated following the methods of Gao et al. (2011). The total lipid extract (TLE) was split into a acid and neutral fractions using aminopropyl silica gel chromatography with dichloromethane:Isopropanol and 5% glacial acetic acid in ether as eluents. An internal standard (7 μg *cis*-eicosenoic acid) was then added to the acid fraction. Acids were methylated overnight at 60 °C with acidified anhydrous methanol of a known isotopic composition. δD values of individual *n*-acids were later corrected for the isotopic contribution incurred during methylation. Aliphatic compounds were isolated from the neutral fraction by silica gel chromatography with sequential elution by hexane (N1), dichloromethane (N2), and methanol (N4). The N1 fraction was spiked with an internal standard of hexamethylbenzene. A sample blank was analyzed with every batch.

The *n*-alkane and *n*-acid distributions of all samples were determined using an Agilent 6890 gas chromatograph with a flame ionization detector (GC-FID). Compound-specific isotope ratios (δD_{wax}) of long chain (C_{22}-C_{31}) molecules were measured on a Thermo Finnigan Delta + XL isotope ratio mass spectrometer with a HP 6890 gas chromatograph and a high-temperature pyrolysis reactor for sample introduction. For both GC-FID and GC-IRMS analyses, the GC was fit with a 30 m HP1-MS column and the heating protocol was as follows: injector was set to pulsed splitless mode at 320 °C; the oven temperature was held at 70 °C for 1 min, then ramped by 25 °C min^{-1} to 230 °C, then by 6 °C min^{-1} to 315 °C min. The pyrolysis reactor temperature was set to 1445 °C and the flow rate was held constant at 1.4 ml min^{-1}. The H3+ factor was determined every other day and averaged 2.7 ($1\sigma = 0.3$) during the course of analyses. Each sample was measured once on GC-FID and at least twice on GC-IRMS. Isotopic values were accepted if the voltage response was between 2 and 6 volts. A standard mixture containing either C_{16}, C_{18}, C_{22}, C_{26}, and C_{28} *n*-acids or C_{25}, C_{27}, C_{29}, C_{30}, and C_{32} *n*-alkanes was analyzed between every six injections to monitor instrument accuracy, and corrections were made on daily batches for offsets between measured and reported standard values. Analytical uncertainty was calculated using the pooled standard deviation (Eq. (1)). The 1σ uncertainties are reported in Table A1 and are consistently smaller than 3‰.

$$\sigma = \sqrt{\frac{\Sigma(n_i - 1) * s_i^2}{\Sigma(n_i - 1)}}, \tag{1}$$

where i = day for standards and i = sample for samples.

2.3.3. Notation and statistics

The carbon preference index (CPI), a metric of wax degradation and contamination (Bray and Evans, 1961), is calculated using Eqs. (2) and (3), while average change length (ACL) data is calculated using Eq. (4).

$$CPI_{n\text{-}acids} = \frac{2 * \sum_{i=20}^{30} i * C_i (i = evens)}{\sum_{i=19}^{29} i * C_i + \sum_{i=21}^{31} i * C_i (i = odds)}, \tag{2}$$

where i is the carbon number and C is the concentration;

$$CPI_{n\text{-}alkanes} = \frac{2 * \sum_{i=23}^{33} i * C_i (i = odds)}{\sum_{i=22}^{32} i * C_i + \sum_{i=24}^{34} i * C_i (i = evens)} \tag{3}$$

$$ACL = \frac{\sum_{20}^{33} i * C_i}{\sum_{20}^{33} C_i} \tag{4}$$

The isotopic composition of water and waxes is described in delta-notation (Eq. (5)). Hydrogen isotope enrichment factors, ε, were calculated between two reservoirs as in Eq. (6).

$$\delta D\ (‰) = \left(\frac{R_{sample}}{R_{standard}} - 1\right) \times 1000, \tag{5}$$

where $R = \frac{D}{H}$, and the standard is Vienna standard mean ocean water (VSMOW).

$$\varepsilon_{A-B} = \left[\frac{\delta D_A + 1000}{\delta D_B + 1000} - 1\right] * 1000. \tag{6}$$

3. RESULTS

3.1. Plant source water

The $\delta D_{precipitation}$ is most enriched during summer and most depleted during winter (Fig. 2), with a precipitation-weighted mean annual value of −166‰ and a mean summer value of −139‰. The mean annual $\delta D_{precipitation}$ determined by the Online Isotope in Precipitation Calculator is −159‰ (Bowen and Revenaugh, 2003; Bowen, 2015), slightly enriched relative to observations. OIPC modeled monthly values are also somewhat enriched, with a RMSE of 32‰ relative to observations.

In July the surface (0–1 cm) δD_{soil} averages −161.5‰, not significantly different than mean annual $\delta D_{precipitation}$ ($p = 0.27$) whereas in August, surface δD_{soil} is more enriched than annual $\delta D_{precipitation}$ with values averaging

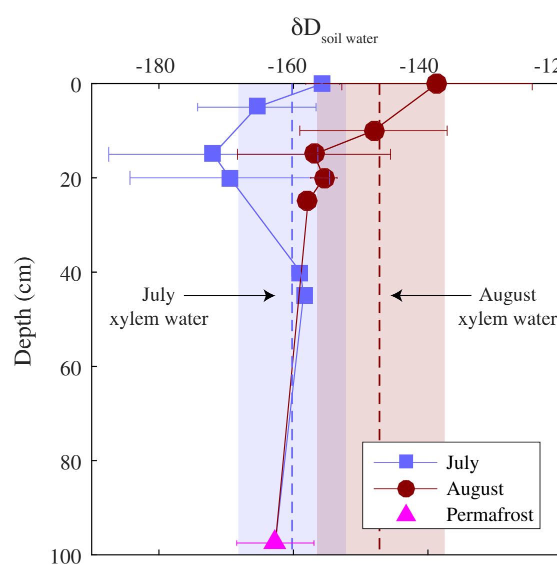

Fig. 3. $\delta D_{soil\ water}$ profiles from July and August. The deep permafrost was sampled in July and is assumed to be constant throughout the year. Error bars are 1σ standard deviation from 1 to 6 replicate field samples; no error bar indicates $n = 1$. Dashed vertical lines are δD_{xylem} from each sampling month (*E. vaginatum* and *B. nana* combined) and the shaded envelopes are 1σ standard deviation of xylem measurements based on multiple plants ($n = 9$ for July, $n = 13$ for August).

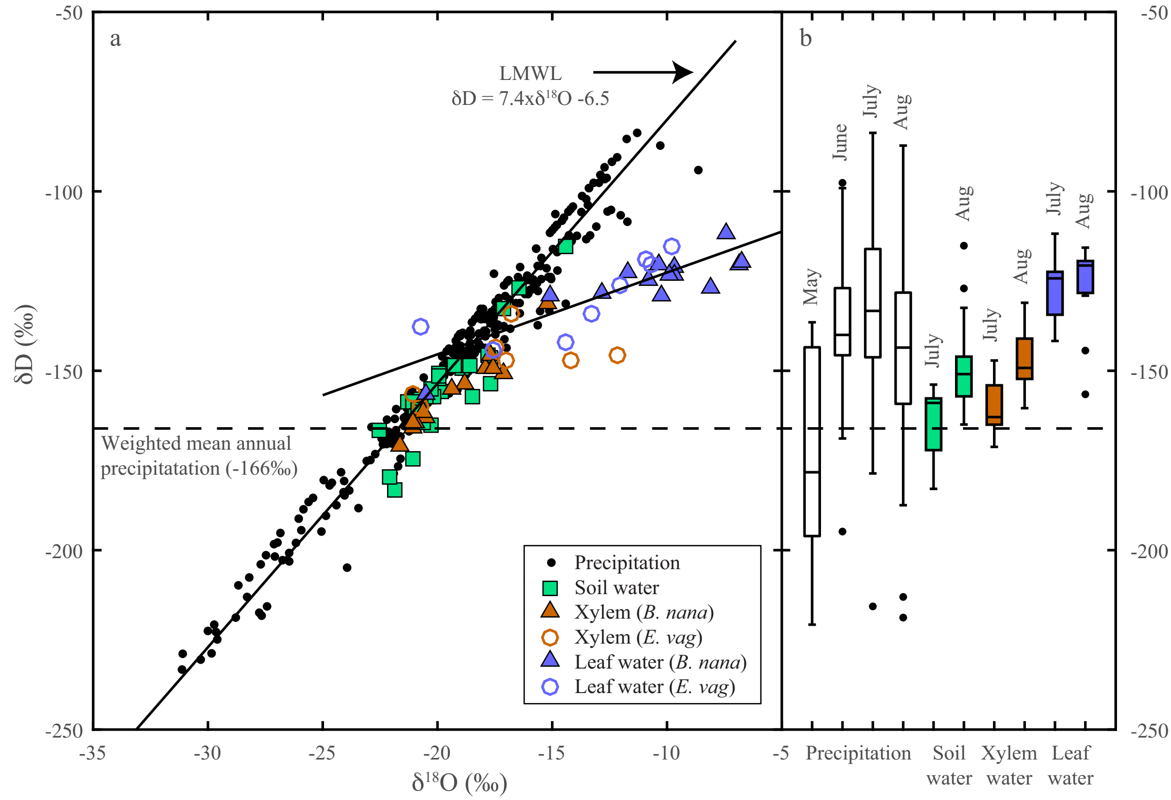

Fig. 4. Panel a: The relationship between δD and $\delta^{18}O$ at Toolik Lake for precipitation (black points), soil water (green squares), plant xylem water of *B. nana* (orange triangles) and *E. vaginatum* (orange circles), and leaf water of *B. nana* (blue triangles) and *E. vaginatum* (blue circles). Nine precipitation isotope measurements were more depleted than shown in the figure, reaching δD values as low as −316‰, but are omitted for clarity. These lower values do not diverge systematically from the LMWL. The second regression line goes through leaf water measurements and illustrates evaporative enrichment in the leaves. Panel b: Summary figure of monthly $\delta D_{precipitation}$, δD_{soil}, δD_{xylem}, and δD_{leaf}. Xylem and leaf water plots combine data from both study species. Boxes represent median, 25th and 75th percentiles, and whiskers extend to most extreme non-outliers. (For interpretation of the references to colour in this figure legend, the reader is referred to the web version of this article.)

−142‰ ($p = 0.0003$) (Fig. 3). Vertical profiles in δD_{soil} also differ between months. In July, there is a shift at intermediate (10–30 cm) depth to values more negative than the permafrost, possibly a result of residual winter precipitation. In contrast, in August there is a steady D-depletion with depth. Permafrost δD_{soil} is assumed to be constant and has a value of −162 ± 6‰, the same as mean annual precipitation ($p = 0.54$). Soil water isotopes fall on the local meteoric water line (LMWL), indicating little effect of soil evaporation (Fig. 4). As such, the progressive enrichment of surface soil water isotopes from July to August likely reflects an increasing contribution of summer rains to the soil water pool.

Xylem water isotopes overlap with the LMWL and with soil water isotopes in $\delta^{18}O$-δD space (Fig. 4), indicating there is little to no fractionation during plant uptake, consistent with previous studies (Ehleringer and Dawson, 1992). Overall, there is no difference in δD_{xylem} between *E. vaginatum* and *B. nana* ($p = 0.084$). The δD_{xylem} increases from −160 ± 8‰ to −147 ± 9‰ between July and August, tracking the enrichment in δD_{soil} (Fig. 5).

Evaporative enrichment increases δD and $\delta^{18}O$ values of leaf water relative to xylem water. The δD_{leaf} is enriched relative to δD_{xylem} by 40 ± 17‰ in *B. nana* and 22 ± 16‰ in *E. vaginatum* (Fig. 4). The intersection between the leaf water δD-$\delta^{18}O$ line and the LMWL can be used to infer the isotopic composition of source water for plant uptake (Polissar and Freeman, 2010), and occurs at $\delta^{18}O = -19$‰ and δD = −148‰. This isotopic composition lies between the July and August xylem water measurements.

3.2. Leaf waxes

3.2.1. Modern plant waxes

Leaves from both *B. nana* and *E. vaginatum* contain *n*-acids from C_{20} to C_{30} and *n*-alkanes from C_{23} to C_{33} (Fig. 6). CPI results show a strong even-over-odd predominance for *n*-acids for both *B. nana* and *E. vaginatum* ($CPI_{B.\ nana} = 14.2 \pm 2.8$; $CPI_{E.\ vaginatum} = 6.3 \pm 1.5$) and vice versa for *n*-alkanes ($CPI_{B.nana} = 7.4 \pm 3.1$; $CPI_{E.\ vaginatum} = 32.3 \pm 8.1$), reflecting the freshness of the sampled leaf waxes. Averaging all *B. nana* samples, we find that even-chain *n*-acids are roughly equally distributed from C_{22} to C_{28}, whereas the *n*-alkane distribution has two peaks at C_{27} and C_{31}. For C_{20}-C_{30} *n*-acids, the average chain length

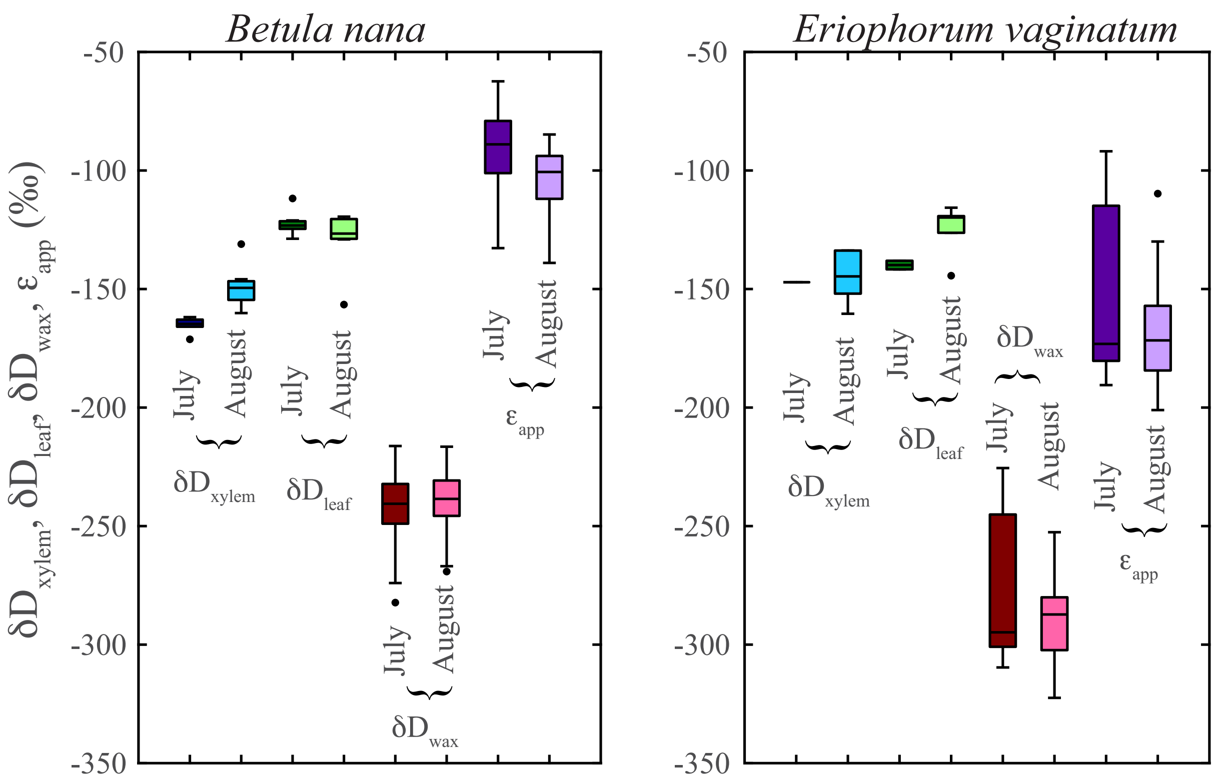

Fig. 5. Hydrogen isotope ratios of plant water and leaf waxes, and the net apparent fractionation between xylem water and leaf waxes for *Betula nana* and *Eriophorum vaginatum* in July and August. δD_{wax} and ε_{app} values represent averages of all measured lipid homologues. The month effect is not significant for values of ε_{app}, but is significant for xylem water in *Betula nana* and leaf water in *Eriophorum vaginatum*.

(ACL) is 24.5 ± 0.7 while for *n*-alkanes, the C_{20}-C_{33} ACL averages 28.7 ± 0.4. *E. vaginatum* lipids are, on average, unimodally distributed and dominated by C_{26} *n*-acid and C_{31} *n*-alkane. ACL averages 24.8 ± 0.5 for *n*-acids and 30.1 ± 0.7 for *n*-alkanes. No difference in ACL was observed between sampling months for either species ($p = 0.59$ for *E. vaginatum* and $p = 0.16$ for *B. nana*). While *B. nana* and *E. vaginatum* have similar concentrations of total *n*-alkanes (1960 μg g leaf^{-1} and 1482 μg g leaf^{-1}, respectively; two-sample *t*-test $p = 0.167$), *B. nana* leaves contained significantly more *n*-acids than *E. vaginatum* (965 μg g leaf^{-1} and 142 μg g leaf^{-1}, respectively; two-sample *t*-test $p = 0.037$).

For isotopic analyses, we focus on the most abundant long chain *n*-acids (C_{22}-C_{30}) and *n*-alkanes (C_{25}-C_{31}). Across all sampling periods, the δD_{wax} of *B. nana* *n*-alkanes and *n*-acids average −232‰ and −248‰, respectively, while *E. vaginatum* *n*-alkanes and *n*-acids average −305‰ and −278‰, thus revealing discernible differences between plant species, but inconsistent differences between lipid classes. Further differences are apparent between homologues (Table 1 and Fig. 7). Calculations of ε_{app} from paired measurements of xylem water and leaf waxes show that ε_{app} is more negative for leaf waxes of *E. vaginatum* (*n*-alkane average: −182‰, *n*-acid average: −154‰) than for waxes of *B. nana* (*n*-alkane average: −89‰, *n*-acid average: −106‰) (Table 1). The difference in fractionation between the two species decreases with decreasing chain length (Fig. 7). Furthermore, we note that ε_{app} is less negative during July than August sampling, particularly for *E. vaginatum* (Fig. 5).

3.2.2. Sedimentary waxes

Sediment traps in Lake E5 collected between 0.05 and 0.3 g of solids during the deployment periods, equivalent to a mass flux of 0.1–0.85 g m^{-2} d^{-1}. The concentration of *n*-acids (ΣC_{20}-C_{33}) averaged 219 μg g sediment^{-1}, while the concentration of *n*-alkanes (ΣC_{20}-C_{33}) averaged 248 μg g sediment^{-1}. The fluxes of sediment, *n*-acids, and *n*-alkanes peak in June, during and shortly after the spring thaw (Fig. 8), with values of 0.85 g m^{-2} d^{-1}, 230 μg m^{-2} d^{-1}, and 304 μg m^{-2} d^{-1}, respectively. The carbon preference index of sediment trap waxes ($CPI_{n\text{-acids}} = 2.7 \pm 1.3$; $CPI_{n\text{-alkanes}} = 3.1 \pm 2.9$) are lower than the waxes from live vegetation, but still show strong even/odd differences that reflect the relatively low degradation state of the waxes (Fig. 6). The *n*-acids exhibit a unimodal distribution with a peak at the C_{24} homologue and an ACL of 23.3 ± 0.7. The *n*-alkanes are bimodal with peaks at C_{20} and C_{27}, and have an ACL of 25.2 ± 1.5. The low abundance of waxes required that sediment trap replicates be composited into early and late summer samples for isotope analysis. In Lake E5, $\delta D_{C28\text{-acid}}$ varies by 15‰ throughout the summer, ranging from −256‰ in May/June and August/September to −243‰ in July (Fig. 8). The flux-weighted input of C_{28} *n*-acid during the summer has a δD value −253.7‰, which is

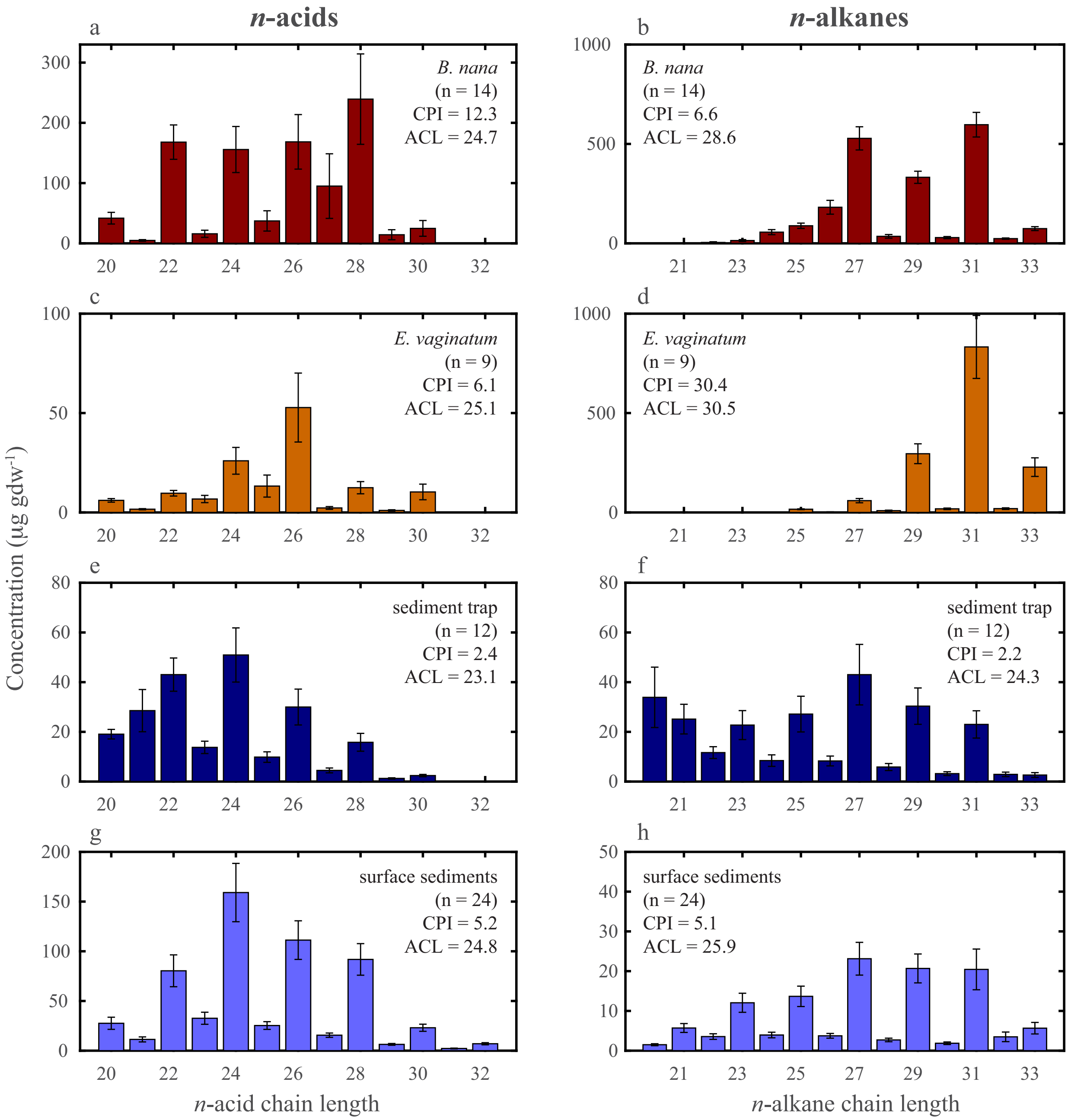

Fig. 6. Concentration of long chain *n*-acids (C_{20}-C_{32}) and *n*-alkanes (C_{20}-C_{33}) in live specimens of *Betula nana* (panels a and b), *Eriophorum vaginatum* (panels c and d), sediment trap samples in Lake E5 (panels e and f), and surface sediments from lakes around Toolik Field Station (panels g and h). For plant samples, concentrations are given relative to grams of dry leaf material, and for sediments it is relative to grams of dry sediment. Error bars represent standard error of the mean, while the *n* represents the total number of vegetation, sediment trap, and surface sediment samples.

indistinguishable from the C_{28} *n*-acid in Lake E5 surface sediment of −254.8‰.

In Toolik Lake, sediment flux and lipid fluxes were lower than in Lake E5, such that wax abundance was too low for isotope analysis. The maximum sediment collected was 0.05 g, and the maximum sediment flux was 0.05 g m^{-2} d^{-1}. The concentration of *n*-acids (C_{20}-C_{30}) averaged 226 μg g sediment^{-1} while the concentration of *n*-alkanes (C_{23}-C_{33}) averaged 438 μg g sediment^{-1}. Lipid distributions were similar between the two lakes.

Like sediment trap samples, the C_{24} *n*-acid is the most abundant wax homologue in surface sediments from all lakes. The ACL for *n*-acids is 24.8 ± 0.8 and the CPI is 5.2 ± 1.0 in the lake sediment samples, consistent with a terrestrial plant wax origin. The C_{27} to C_{31} are the most abundant *n*-alkanes and present in roughly equal

Table 1
The average δD_{wax} (‰) and net apparent fractionation (‰) of leaf waxes on living plants from all sites for each sampling date. Standard deviations in parentheses reflect variance between field samples, and n is the number of samples collected with each effort. Fractionation is calculated using paired xylem water measurements leaf wax measurements for each sample. Dashes mean not available.

		Xylem water	*n*-acids					*n*-alkanes			
			C_{22}	C_{24}	C_{26}	C_{28}	C_{30}	C_{25}	C_{27}	C_{29}	C_{31}
B. nana											
δD (1σ)	Aug 6, 2013 ($n = 1$)	−131 (–)		−252 (–)	−243 (–)	−246 (–)		−245 (–)	−228 (–)	−216 (–)	
	July 17/19, 2014 ($n = 7$)	−165 (3)	−271 (7)	−252 (8)	−242 (5)	−238 (7)	−252 (3)		−239 (6)	−227 (7)	−232 (7)
	Aug 7/8, 2014 ($n = 6$)	−152 (5)	−263 (6)	−245 (3)	−240 (6)	−237 (7)	−235 (8)	−243 (9)	−238 (5)	−228 (4)	−229 (5)
	Average ($n = 14$)	−156 (11)	−267 (7)	−248 (7)	_241 (5)	−238 (7)	−244 (11)	−243 (7)	−237 (6)	−227 (6)	−231 (6)
ε_{app} (1σ)	Aug 6, 2013			−139 (–)	−129 (–)	−132 (–)		−130 (–)	−112 (–)	−98 (–)	
	July 17/19, 2014		−123 (6)	−100 (6)	−90 (9)	−85 (10)	−101 (–)		−87 (6)	−72 (8)	−78 (8)
	Aug 7/8, 2014		−131 (6)	−109 (4)	−104 (7)	−100 (9)	−95 (1)	−104 (3)	−101 (4)	−89 (4)	−90 (4)
	Average		−127 (7)	−108 (12)	−100 (13)	−96 (16)	−97 (4)	−113 (15)	−96 (10)	−82 (12)	−84 (9)
E. vaginatum											
δD (1σ)	Aug 6, 2013 ($n = 2$)	−134 (–)		−282 (1)	−298 (1)	−285 (1)					
	July 17/19, 2014 ($n = 3$)	−150 (5)	−248 (–)	−243 (25)	−259 (35)	−272 (24)	−295 (7)			−296 (2)	−303 (6)
	Aug 7/8, 2014 ($n = 4$)	−150 (8)	−267 (20)	−278 (6)	−290 (4)	−283 (4)	−295 (14)			−308 (6)	−309 (9)
	Average ($n = 9$)	−145 (9)	−266 (20)	−272 (21)	−282 (27)	−278 (13)	−296 (12)			−303 (8)	−308 (8)
ε_{app} (1σ)	Aug 6, 2013			−171 (1)	−189 (2)	−174 (1)					
	July 17/19, 2014		−108 (–)	−108 (22)	−127 (34)	−142 (21)	−170 (15)			−171 (3)	−180 (11)
	Aug 7/8, 2014		−136 (28)	−150 (9)	−170 (7)	−161 (6)	−170 (13)			−189 (5)	−187 (10)
	Average		−136 (28)	−148 (27)	−164 (36)	−160 (19)	−172 (12)			−183 (9)	−186 (8)

Table 2
Location, depths, and watershed characteristics of the 24 lakes from which we sampled surface sediment. S: Sagavanirktok (>125 ka), IK I: Itkillik I (~60 ka), IK II: Itkillik II (25–11.5 ka), IK-mix: mix of IK I and IK II. The sum of watershed cover classes are less than one because not shown is the area covered by lakes.

Lake Name	Lat.	Long.	Glacial Surface	Mean Depth (m)	Watershed area (ha)	Vegetation types (fraction of watershed)							
						Barren	Dry tundra	Snowbed	Moist non-acidic tundra	Moist acidic tundra	Shrub tundra	Riparian shrubland	Wetland
UCL	68.629	−149.413	S	–	264	0.01	0.06	0	0.02	0.42	0.07	0.38	0.03
E5	68.643	−149.458	S	6.3	129	0	0.21	0	0	0.69	0.01	0	0
E6	68.644	−149.439	S	1.6	26	0	0.21	0.34	0	0.37	0	0	0
E1	68.626	−149.554	IK I	3.1	87	0.13	0.17	0.04	0.16	0.32	0	0.14	0
I6HW	68.581	−149.619	IK I	3.6	56	0	0.13	0.07	0.31	0.16	0.23	0	0.01
Fog1	68.684	−149.079	IK II	8.4	22	0	0.06	0.07	0	0.75	0	0	0
Fog2	68.679	−149.089	IK II	7.8	37	0	0.27	0	0	0.58	0	0	0
Fog4	68.680	−149.072	IK II	2.1	55	0	0.23	0.08	0.02	0.59	0	0	0
Galbraith	68.460	−149.420	IK II	4.2	–	–	–	–	–	–	–	–	–
I1	68.569	−149.588	IK II	3.9	133	0	0.06	0	0.16	0.53	0.04	0.01	0.03
I2	68.571	−149.566	IK II	7.2	97	0	0.03	0	0.06	0.77	0	0.06	0
I3	68.575	−149.581	IK II	1.8	343	0	0.04	0	0.11	0.65	0.04	0.04	0.02
I4	68.580	−149.583	IK II	3.0	421	0	0.04	0	0.10	0.66	0.04	0.05	0.02
I5	68.587	−149.590	IK II	3.9	597	0	0.05	0	0.07	0.69	0.03	0.04	0.01
I6	68.597	−149.593	IK II	5.7	924	0	0.06	0.01	0.11	0.63	0.04	0.05	0.01
I7	68.601	−149.593	IK II	3.7	965	0	0.08	0	0.11	0.60	0.04	0.05	0.01
I8	68.610	−149.582	IK II	2.7	2970	0.03	0.12	0.03	0.12	0.45	0.12	0.09	0.03
Iswamp	68.611	−149.597	IK II	2.3	1227	0	0.11	0	0.12	0.57	0.03	0.07	0.02
N1	68.640	−149.604	IK II	4.8	32	0	0.53	0	0.22	0.05	0	0	0.04
N2	68.641	−149.622	IK II	5.0	21	0	0.28	0.20	0.07	0.31	0	0.07	0
S11	68.631	−149.648	IK II	3.3	24	0	0.36	0.03	0	0.54	0	0.04	0
S6	68.630	−149.639	IK-mix	3.0	796	0.02	0.29	0.08	0.35	0.14	0.04	0.03	0
S7	68.630	−149.643	IK-mix	0.8	40	0	0.44	0.1	0.13	0.33	0	0.03	0
TLK	68.632	−149.602	IK-mix	7.4	6486	0.02	0.16	0.2	0.15	0.42	0.07	0.08	0.02

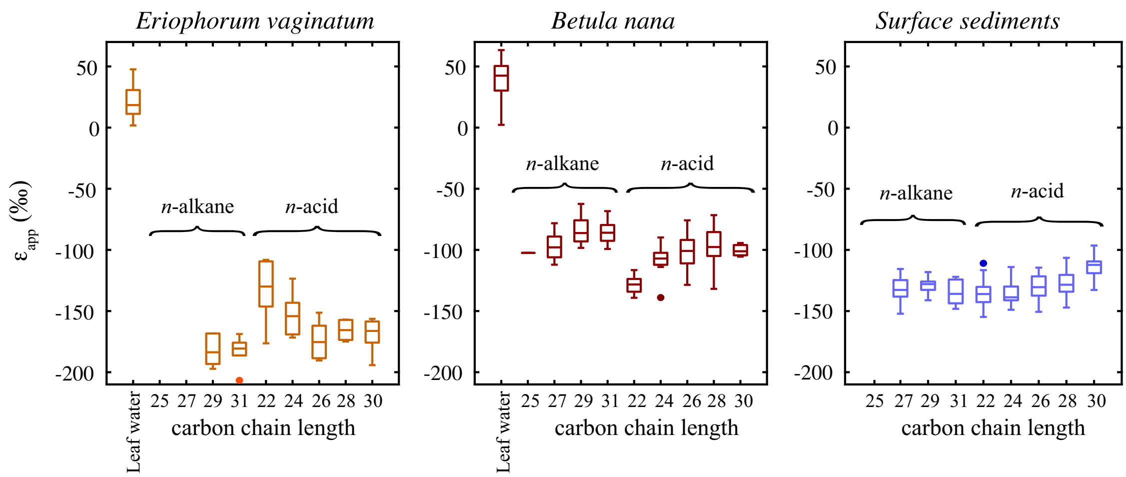

Fig. 7. Net apparent D/H fractionation (ε_{app}) for (a) *Eriophorum vaginatum* (C_3 monocot; $n = 9$), (b) *Betula nana* (C_3 shrub; $n = 14$), and (c) lake surface sediments ($n = 24$). For plant samples, fractionation is calculated relative to paired xylem water measurements, while for surface sediments, source water is set to the average of all xylem water measurements (−153‰). Boxes represent median, 25th and 75th percentiles, and whiskers extend to most extreme non-outliers.

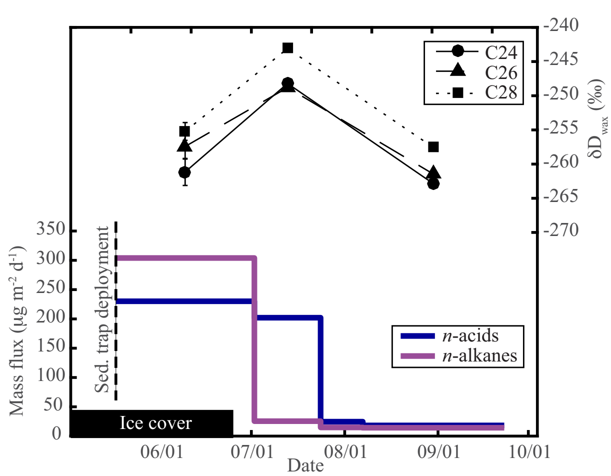

Fig. 8. *n*-acid and *n*-alkane fluxes and δD_{wax}, measured in sediment traps deployed in Lake E5 in 2014. Each point represents an average of 14–46 days of sediment collection. D/H ratios were measured on *n*-acids only, and are not available for the third collection because of insufficient sample mass. δD_{wax} error bars are standard deviation of 3 sediment traps, but traps were composited prior to analysis for the later sampling dates.

abundances. The ACL and CPI for *n*-alkanes average 27.2 ± 0.4 and 5.0 ± 0.8, respectively. Similar to observations from the nearshore Beaufort Sea (Drenzek et al., 2007), *n*-acids are more abundant than *n*-alkanes. The δD_{wax} of lipids in surface sediments averages −264.5 ± 7.1‰ for all measured *n*-alkanes and −261.3 ± 11.0‰ for all measured *n*-acids and has a range of 49‰ (Table 3) across all lakes and lipid homologues.

To calculate a watershed-scale ε_{app}, we compared the δD_{wax} of lake surface sediments from 24 lakes to the δD of plant source water. We provide three estimates of ε_{app}, based on different estimates of $\delta D_{source\ water}$. Using precipitation-weighted mean annual $\delta D_{precipitation}$ (−166‰), ε_{app} averages −118 ± 9‰ for *n*-alkanes and −114 ± 13‰ for *n*-acids. Using precipitation-weighted mean summer $\delta D_{precipitation}$ (−139‰), ε_{app} averages −146 ± 8‰ for *n*-alkanes and −142 ± 13‰ for *n*-acids. Using the average δD_{xylem} values measured in this study (−153‰), ε_{app} averages −132 ± 8‰ for *n*-alkanes and −128 ± 13‰ for *n*-acids. Values of ε_{app} tend to be slightly more negative for smaller carbon number homologues than larger homologues (Fig. 7). Our estimates of sedimentary wax ε_{app} suggest that *n*-alkanes are more strongly fractionated relative to source water than are *n*-acids – the C_{29} *n*-alkane is depleted by 15‰ relative to C_{30} *n*-acid (paired *t*-test, $p < 0.0001$), while C_{27} *n*-alkane is just 4‰ depleted relative to C_{28} *n*-acid (paired *t*-test, $p = 0.060$). Thus while our plant samples exhibited opposing offsets between *n*-alkanes and *n*-acids, the sedimentary waxes are in general agreement with expectations from previous work on individual plants (Chikaraishi and Naraoka, 2007; Hou et al., 2007) and marine sediments (Li et al., 2009).

3.3. Vegetation effects on apparent fractionation

Isotopic differences between study lakes most likely arise from watershed-scale differences in soil water evaporation and/or plant distributions. Due to limited evidence for evaporative fractionation observed in our soil samples, large observed differences in ε_{app} between plant types, and the large variation in plant types across watersheds (Table 2), vegetation is likely the primary cause of the large ε_{app} variability (Table 2). Based on single and multi-variate regressions, we find that the best predictor of ε_{app} for nearly all wax homologues is the relative abundance of barren and dry tundra vegetation. While barren tundra (bedrock) is dominated by lichens, the dry tundra is dominated by eudicot shrubs and forbs such as *Salix spp.* The positive correlation is consistent with the hypothesis that greater eudicot cover should result in less negative ε_{app}. In contrast, the abundance of moist and shrub tundra, which contain an

Table 3
δD_{wax} and apparent fractionation (‰) of lake surface sediments. Fractionation is calculated using a source water value of −153‰ based on xylem water observations for the two plant species. Dashes mean not measured.

Lake name	Lat.	Long.	*n*-acids					*n*-alkanes		
			C_{22}	C_{24}	C_{26}	C_{28}	C_{30}	C_{27}	C_{29}	C_{31}
UCL	68.629	−149.413	–	–	−270	−265	–	–	–	–
E5	68.643	−149.458	−268	−263	−253	−255	−246	−258	−261	
E6	68.644	−149.439	−268	−270	−250	−248	−235	−269	−266	−258
E1	68.626	−149.554	−260	–	−265	−262	−256	−259	−259	−257
I6HW	68.581	−149.619	−265	−271	−262	−260	−248	−260	−263	−268
FOG1	68.684	−149.079	−268	–	−267	−263	−248	−255	−257	−267
FOG2	68.679	−149.089	−265	−264	–	−259	–	−257	−259	−258
FOG4	68.680	−149.072	−284	–	−269	−263	–	−266	−264	−271
GALBRAITH	68.460	−149.420	−267	−262	−260	−262	−246	–	–	–
I1	68.569	−149.588	−279	−277	−257	−256	−243	−261	−260	−271
I2	68.571	−149.566	–	−271	−256	−260	−246	–	–	–
I3	68.575	−149.581	−272	–	−278	−275	−256	−270	−265	−278
I4	68.580	−149.583	−272	–	−269	−268	−254	−266	−264	−278
I5	68.587	−149.590	−272	–	−262	−266	−253	−271	−268	−275
I6	68.597	−149.593	−262	–	−266	−268	−255	−270	−265	−270
I7	68.601	−149.593	−284	−279	−270	−270	–	−271	−269	−277
I8	68.610	−149.582	−274	−273	−268	−267	−254	−265	−260	−275
ISWAMP	68.611	−149.597	−278	–	−281	−278	−265	−282	−273	−268
N1	68.640	−149.604	−253	–	−254	−247	−243	−256	−255	−256
N2	68.641	−149.622	−252	–	−251	−244	−251	−251	−253	−262
S11	68.631	−149.648	–	−250	−256	−255	–	–	–	–
S6	68.630	−149.639	−247	–	−250	−243	−235	−259	−261	–
S7	68.630	−149.643	−274	–	−269	−267	−247	−270	−261	−257
TLK	68.632	−149.602	–	–	–	−254	–	–	–	–
Average δD_{wax} (1σ)			−268 (10)	−268 (9)	−263 (9)	−261 (9)	−249 (8)		−264 (8)	−262 (5)
Average ε_{app} (1σ)			−136 (12)	−136 (10)	−130 (10)	−127 (11)	−113 (9)		−131 (9)	−129 (6)

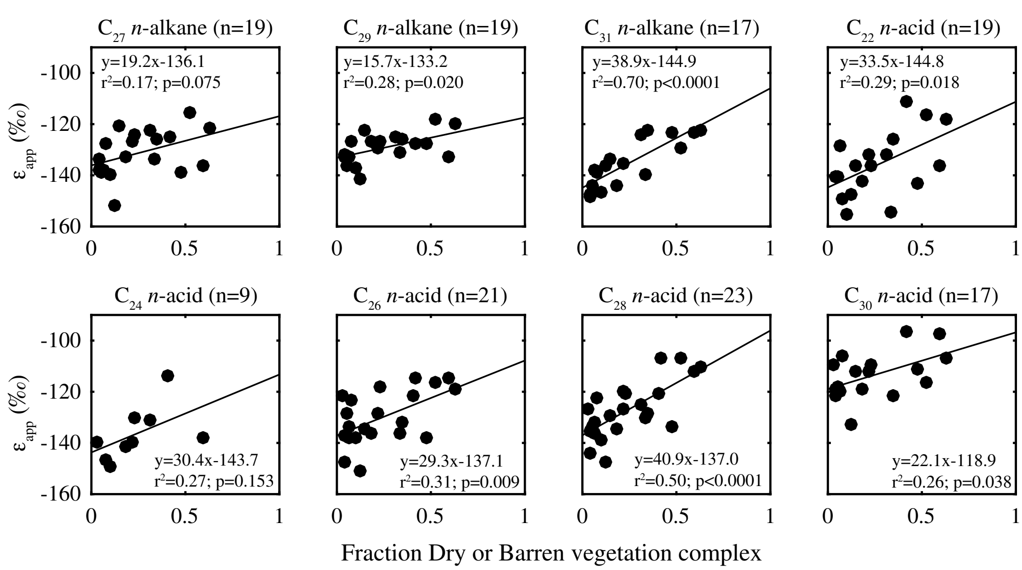

Fig. 9. The relationship between surface sediment ε_{app} and the relative area of each watershed comprised of dry or barren tundra (Alaska Geobotany Center, http://www.arcticatlas.org/). Dry and barren tundra are dominated by shrubs and forbs and have shallow organic soil layers (Walker et al., 1994). Fractionation factors are calculated using a source water isotopic composition of −153‰, the average of all xylem water measurements.

abundance of moss and the sedges *Eriophorum* spp. and *Carex* spp., is negatively correlated with ε_{app} (Fig. 9, Table A2).

4. DISCUSSION

4.1. Apparent fractionation in the Alaskan Arctic is similar to temperate and tropical settings

A pressing question in the application of leaf wax hydrogen isotopes for paleoclimate reconstructions is whether apparent D/H fractionation is affected by enhanced transpiration in polar regions due to 24-h photosynthesis, as suggested by previous studies (Yang et al., 2011; Shanahan et al., 2013; Porter et al., 2016), or, if there is little effect of latitude on ε_{app} as recently suggested by Liu et al. (2016). Our study site is within the Arctic circle (68 °N), at a similar latitude to previous studies on sub-Arctic and Artic leaf wax fractionation, which are here considered those studies above 63 °N (Sachse et al., 2006; Yang et al., 2011; Wilkie et al., 2012; Shanahan et al., 2013; Porter et al., 2016). We find that ε_{app} of Arctic *n*-alkanes and *n*-acids are generally similar to those observed at mid- and low-latitude locations (Sachse et al., 2004; Hou et al., 2007; Garcin et al., 2012), suggesting that the effect of 24-h photosynthesis is of limited importance and that the fundamental controls on ε_{app} in the Arctic are similar to those in temperate and tropical regions, with the exceptions that the Arctic is differentiated by its extremely short growing season, unique flora, and the presence of permafrost.

With the exception of the study by Yang et al. (2011), our estimates of ε_{app} at the plant scale are in general agreement with results from plants of the same growth forms from regions both with and without a summer diel light cycle. For example, across a latitudinal transect which included 24-hour daylight sites, Sachse et al. (2006) found that *Betula pubescens* and *B. pendula* exhibited $\varepsilon_{alkane\text{-}water}$ of −138 to −86‰, a range which brackets our estimate of −108‰ for the closely related *B. nana*. Sachse et al. (2006) did not observe a consistent latitudinal effect on ε_{app} within either *Betula* species, which would also suggest day length has little effect on ε_{app}. The average *n*-acid D/H fractionation for *B. nana* specimens at our site ($\varepsilon_{acid\text{-}water} = -89‰$) falls within the range reported for a variety of eudicot plants ($\varepsilon_{acid\text{-}water} = -156$ to $-85‰$) collected from a mid-latitude site in Massachusetts, USA by Hou et al. (2007). The Alaskan $\varepsilon_{alkane\text{-}water}$ (−105‰) is at least 10‰ enriched compared to Massachusetts specimens ($\varepsilon_{alkane\text{-}water} = -180$ to $-115‰$), and slightly enriched relative to the ε_{app} of −117‰ reported for C_{27} *n*-alkanes of dominant shrub taxa in western Greenland (Thomas et al., 2016). Fractionation values for *E. vaginatum* ($\varepsilon_{alkane\text{-}water} = -182‰$ and $\varepsilon_{acid\text{-}water} = -153‰$) fall within the ranges for other graminoids reported by Hou et al. (2007) ($\varepsilon_{alkane\text{-}water} = -206$ to 154‰ and $\varepsilon_{acid\text{-}water} = -195$ to $-148‰$). Our results also overlap with ε_{app} measurements from living plants in Arctic Siberia, where Wilkie et al. (2012) report ε_{app} values ranging from −135 to −97‰ for *n*-acids from seven tundra species, comprising both eudicots and monocots. Unlike at our sampling sites, however, Wilkie et al. (2012) did not observe a significant D-depletion in monocots relative to eudicots. This between-site difference may arise because, while *Eriophorum* in the Toolik Lake region is found primarily in mesic soils, *Poaceae*, the monocot studied by Wilkie et al. (2012), can be found across diverse soil types in the Arctic (Oswald et al., 2003) and may be more susceptible to evaporation effects on D/H ratios.

In our study region, the ecosystem-scale ε_{app} inferred from waxes in lake sediments averages −132‰ for *n*-alkanes and −128‰ for all *n*-acid homologues when the average δD_{xylem} is used as a baseline for source water. The average source water δD value is undoubtedly a mix of precipitation across seasons, and as discussed below, is likely biased towards summer values in the Arctic. The δD_{xylem} values reported here represent a snapshot in mid-summer and may be unique to the plant species studied here. Nonetheless, because the soil thaw layer is shallow (<50 cm), plants are generally drawing water from the same pool. The δD_{xylem} may also be enriched relative to xylem waters in May/June when leaf flush occurs, thereby biasing ε_{app} to be slightly less negative than the growing-season average. Nonetheless, the application of δD_{xylem} as an estimate of source water is justified for a few reasons. First, the presence of some residual cold season (D-depleted) water in soil profiles implies that mean summer $\delta D_{precipitation}$ as a source water would over estimate $\delta D_{source\ water}$, while using a mean annual $\delta D_{precipitation}$ would likely underestimate $\delta D_{source\ water}$ because it would not account for the summer bias in the growing season. Because the xylem water estimates fall intermediate between mean annual and mean summer rainfall, we propose that the δD_{xylem} measurements provide the most reasonable baseline value of the source water. While better constraining the δD_{xylem} during the period of leaf flush would further aid the assessment of source water seasonality, the δD_{wax} of newly formed leaves is more dependent on the D/H ratios of stored carbohydrates and NADPH than on xylem waters (Newberry et al., 2015), and so spring δD_{xylem} is not critical in this analysis.

The ecosystem-scale ε_{app} values are intermediate between our estimates of ε_{app} from *B. nana* and *E. vaginatum*, and, for *n*-acids, slightly more negative than the ε_{app} estimate of −110.5‰ in Arctic Siberia (Wilkie et al., 2012). The ε_{app} estimates for long chain (C_{27}, C_{29}, C_{31}) *n*-alkanes in northern Alaska fall within the range of −141 to −122‰ found in high latitude lakes of Europe (Sachse et al., 2004). Our estimates are slightly more negative than those reported from southern USA, where the C_{26}-C_{30} *n*-acids exhibit ε_{app} values of −98 to −102‰ relative to precipitation (Hou et al., 2008), but more positive than a report from West Africa, where ε_{app} for C_{29} and C_{31} *n*-alkanes was between −168 and −142‰. Regardless of the comparison with the tropics, our estimates are dramatically more negative than the ε_{app} estimates of −55 to −60‰ for both *n*-alkanes and *n*-acids from some prior work in sub-Arctic and Arctic sites (Shanahan et al., 2013; Porter et al., 2016).

We postulate that the large discrepancy in ε_{app} between our study and previous Arctic field studies derives from differences in the assumed seasonality and estimated isotope compositions of plant source waters. Some prior studies that found small Arctic ε_{app} use source water δD values estimated to represent mean annual $\delta D_{precipitation}$ (Yang et al., 2011; Shanahan et al., 2013; Porter et al., 2016). For the Baffin Island study (Shanahan et al., 2013), this assumption is compounded with the use of estimated rather than measured $\delta D_{precipitation}$ values, as well as low humidity and a predominance of dicotyledonous species (forbs) in their study area, all of which might reduce apparent D/H fractionation. In Central Canada, Porter et al. (2016) calculated ε_{app} of −59‰ by comparing fossil waxes to mean annual precipitation preserved in pore ice. However, it is unclear whether pore ice records water frozen *in situ* at the same time and in the same season as that when the plant waxes were formed. Moreover, application of this ε_{app} value to δD_{wax} of modern soils in their study area (Pautler et al., 2014) results in an underestimation of modern mean annual $\delta D_{precipitation}$ by 28‰ and a resulting underestimation of modern mean annual temperature by 13 °C (Porter et al., 2016). While it is possible that source water for plants can partially come from snowmelt (Alstad et al., 1999; Leffler and Welker, 2013), the ground is often frozen during the season of snow melt and water from snowmelt in Arctic spring is mostly lost through runoff. It is more likely that the fossil pore water isotopes used by Porter et al. (2016) reflect cold season (D-depleted) precipitation rather than precipitation during the plant growing season (D-enriched) (Blok et al., 2015).

Low apparent fractionation values have been previously explained by the 24-h sunlit conditions that characterize the Arctic summer, which allow photosynthesis throughout the 24-h day that might drive strong isotopic fractionation of leaf waters due to 24-h evaporation. This hypothesis is supported by greenhouse experiments that indicate ε_{app} values from −87 to −62‰ for plants grown in 24-h light conditions (Yang et al., 2009). These values are difficult to explain. It is possible that the exceptionally small fractionation values that Yang et al. (2009) observed partly resulted from their choice of study species – *Metasequoia, Larix*, and *Taxodium* are expected to exhibit relatively small ε_{app} values based on their phylogenetic lineages (Gao et al., 2014a). Thus, in cases where arctic forests are dominated by these conifers, a reduced fractionation value may be appropriate for calculating ancient $\delta D_{precipitation}$ from ancient δD_{wax}. Nonetheless, for the modern arctic tundra plants studied here, our data argue against a 24-h photosynthesis effect of leaf water isotopes.

Direct observations of $\varepsilon_{leaf\text{ - }xylem}$ do not indicate that continuous daylight has a significant impact on δD_{wax}. Although evaporative enrichment at the leaf surface increases δD_{leaf} relative to δD_{xylem} (Roden and Ehleringer, 1999; Tipple et al., 2015), the magnitude of this enrichment observed at Toolik (40‰ and 21‰ for *B. nana* and *E. vaginatum*, respectively) is within the range of isoscape model predictions for Alaska (Kahmen et al., 2013a). The observed enrichment of leaf water over xylem water is also similar to field and growth chamber observations in temperate environments (Massachusetts and New York) with diel light cycles and relative humidity similar to where Gao et al. (2014a) found that $\varepsilon_{leaf\text{ - }xylem}$ is slightly greater for eudicots (34 ± 13‰) than *Poales* (20 ± 11‰). We hypothesize that the species difference in δD_{leaf} may result from differences in plant height and leaf physiology, with *B. nana* somewhat taller and more susceptible to leaf water enrichment due to a longer flow path of water during transpiration (Gao and Huang, 2013). Regardless of the differences between plant types, both plant water isotope measurements show little effect of continuous daylight on leaf water isotopes, and by extension, net apparent fractionation.

While leaf water measurements are useful for assessing the importance of evaporative enrichment, leaf waters can display large diel isotope variations (Flanagan and Ehleringer, 1991) which were not captured in our sampling scheme. To circumvent the uncertainties of spot sampling, we further tested the effect of changing leaf transpiration on the isotope values of leaf water using the modified Craig-Gordon model for leaf water (Flanagan and Ehleringer, 1991; Tipple et al., 2015). This model calculates the isotopic composition of water at the site of evaporation, rather than water in the bulk leaf tissue, which can also contain a fraction of unevaporated xylem water. Nevertheless, the model can qualitatively describe the potential impact of diel or continuous transpiration on leaf water isotope enrichment. Using average JJA meteorological conditions from Toolik Field Station (Toolik Environmental Data Center Team, 2016), and atmospheric vapor δD at Toolik (Klein et al., 2015), we modeled δD_{leaf} for the range of transpiration rates of Arctic grasses (Gebauer et al., 1998). We find that δD_{leaf} decreases with increasing transpiration rates, but the overall variation is small, less than 1‰ (Fig. 10). These model results support the findings of

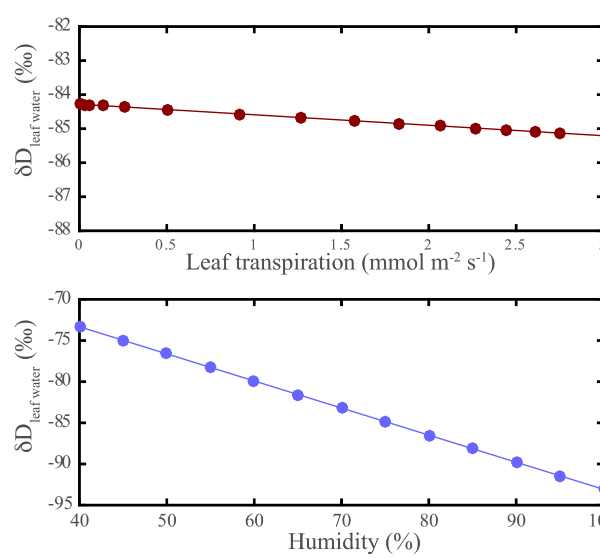

Fig. 10. Modeled leaf water isotopes under varying (a) transpiration and (b) humidity conditions. The model used in this sensitivity analysis was developed by Tipple et al. (2015) and uses JJA meteorological inputs from Toolik Lake Field Station (Toolik Environmental Data Center Team, 2016), an initial source water isotope value of −153‰ (this study), and atmospheric vapor δD measured at Toolik Lake (Klein et al., 2015).

Sullivan and Welker (2007), who demonstrated that, for arctic willow (*Salix arctica*), increasing transpiration results in lower, not higher, leaf water $\delta^{18}O$. Furthermore, findings of Roden and Ehleringer (1999) indicate that leaf water at the site of evaporation reaches isotopic equilibrium within two hours under constant evaporation, and so prolonged (24 h) transpiration should not lead to anomalously enriched leaf water isotope values. Thus, our modeling and prior observational data suggest that 24-h transpiration in the Arctic would, if anything, decrease δD_{leaf} and thereby make ε_{app} more negative, rather than the opposite.

Model results also suggest a relatively small humidity effect on leaf water isotopes. For a 1% increase in relative humidity, δD_{leaf} decreases by 0.33‰ (Fig. 10). Based on the $\delta D_{precipitation}$-temperature relationship of 3.1‰°C^{-1} reported by Porter et al. (2016), this equates to approximately a 1 °C inferred temperature change per 10% change in relative humidity. As such, the effect of humidity change on δD_{wax} interpretations may be relatively insignificant in the Arctic.

The ε_{app} values for leaf waxes from *E. vaginatum* and *B. nana* align well with previous studies that find waxes in graminoids are D-depleted relative to those from forbs, shrubs, and trees (Sachse et al., 2012; Gao et al., 2014a; Liu et al., 2016) and that waxes in monocots are depleted relative to eudicots (Gao et al., 2014a). Interestingly, however, fractionation values for the shorter chain length *n*-acids (C_{24} and C_{26}) were similar for our two study species. This result suggests that shorter chain lengths may be more resilient to vegetation effects in the geologic record. However, with the knowledge that other species, particularly *Sphagnum* moss (Nichols et al., 2009) and aquatic macrophytes (Gao et al., 2011), contribute substantial C_{24} *n*-acid and other short-chain waxes to lake sediments, it remains uncertain if this finding can be extrapolated across all relevant plant types.

It is possible that D/H fractionation in this study is overestimated (more negative than true ε_{app}), due to seasonally biased sampling of waxes and source waters. To evaluate this, we consider a wider range of possible source water δD values. For sedimentary waxes in Toolik and the surrounding lakes, if the plant source water is equal to the mean annual $\delta D_{precipitation}$ (−166‰) rather than summer xylem water (−153‰), ε_{app} ranges from −99‰ for C_{30} *n*-acid to −122‰ for C_{22} and C_{24} *n*-acids. This is still similar to ε_{app} in non-polar regions (Sachse et al., 2004; Hou et al., 2008) and very different from the small values observed at Baffin Island and Central Canada (Shanahan et al., 2013; Porter et al., 2016). To generate ε_{app} as small as −60‰ at our site, it is necessary to invoke source water δD values of −213‰. Such a strong winter-biased source water isotope value is unlikely considering that δD_{xylem} during the growing season averaged −153‰, that 60% of annual precipitation occurs in the three summer months, and that most of the snowmelt is lost as runoff during the spring thaw (Woo, 2012).

4.2. Constraining the seasonality of δD_{wax} signals in the Arctic

It is challenging to accurately identify the isotope value of the source water involved in plant wax synthesis in the Arctic because of the extreme seasonal changes in $\delta D_{precipitation}$ and the uncertainty surrounding the timing of leaf wax synthesis. For our location, we estimate that the δD of source water used for plant growth averages −153‰, based upon both direct measurements of xylem water as well as the intersection between the leaf evaporation line with the LMWL (Fig. 4). Although soil and xylem water collections occurred during peak seasonal warmth and peak $\delta D_{precipitation}$, their isotopic composition was intermediate between the mean annual amount-weighted $\delta D_{precipitation}$ (−166‰) and the summer $\delta D_{precipitation}$ (JJA average = −139‰.) In regions of continuous permafrost, soil infiltration of snowmelt is variable, but generally inhibited during cold months by the impermeability of soil ice (Woo, 2012). As a result, considerable snowmelt is lost as surface runoff and the spring/summer soil water during the period of leaf flush is mostly composed of spring (May and June) precipitation. The predominance of growing-season precipitation over cold-season precipitation in surface soil waters is evident in both July and August, as the δD_{soil} is isotopically similar to spring and summer rains (Fig. 4). Nevertheless, δD_{soil} increases from July to August, and, D-depleted water is present at intermediate soil depths in July, which suggest that complete replacement of remnant fall, winter, and spring precipitation requires several weeks to months and that cold-season precipitation, or a mixture of cold- and growing season precipitation, may be available for plant growth. The seasonal change in δD_{soil} profiles seems to have a stronger influence on the δD_{xylem} of *Betula nana*, which as a shrub has a deeper rooting depth than the sedge *Eriophorum vaginatum* (Fig. 5). Indeed, there are indications that snowmelt can contribute over 30% of source water to plants (Ebbs, 2016). Nevertheless, xylem water isotope measurements in this study and another study in Greenland (Sullivan and Welker, 2007) indicate that arctic plants primarily utilize water from the shallow, thawed soil zones, where soil water is isotopically similar to growing season precipitation events (Fig. 3).

The Lake E5 sediment trap results provide additional insight into seasonal variations in the source water that plants use for biosynthesis (Fig. 8). Since the highest flux of waxes to the sediment occurs during the spring freshet, we suggest that waxes entering the lake are primarily produced during previous year(s) and are flushed from soil by snowmelt. There are reports from the Mackenzie River delta and other high-latitude localities that waxes can be pre-aged by years to millennia at the time of deposition (Drenzek et al., 2007). Considering the primary transport mechanism (particulate transport via snowmelt) and lack of degradation inferred from CPI values, we suspect that the majority of waxes entering the lake can be considered recent. The leaf litter reflects the complex integration of the seasonal production, isotopic evolution, and ablation, of waxes from a variety of species. Importantly, the amplitude of the sediment trap δD_{wax} variability throughout the summer (15‰) is greater than we observed in the monthly change in δD_{wax} of living plants, which is surprising, but may be because we did not measure δD_{wax} of plants in the earliest part of the growing season (May or June).

Despite the enrichment of xylem water in August relative to July, δD_{wax} of plants did not change between July and August (Fig. 5). To explain the stable δD_{wax} values, there are multiple plausible scenarios. First, *de novo* wax biosynthesis may have occurred only during the brief period of leaf flush, which occurs in mid-June at our site, as has been reported from greenhouse studies of *Populus trichocarpa* (Kahmen et al., 2011). If this is the case, δD_{wax} would be insensitive to seasonal change in δD_{xylem}; in field settings, however, weeks to months are required for δD_{wax} to stabilize (Newberry et al., 2015) because of a greater need to replenish lost waxes in more harsh conditions. The Lake E5 sediment trap results show seasonal changes in δD_{wax}, implying some seasonal regeneration of waxes (Fig. 8).

In the process of *de novo* wax regeneration during the growing season, δD_{wax} and biosynthetic fractionation at the time of budbreak tend to be less negative than during mid/late-summer because of a greater contribution of D-enriched material from the recycling of stored carbohydrates early in the season (Newberry et al., 2015). Biosynthetic changes during the growing season are also reported to depress mid-summer D/H ratios in saltmarshes (Sessions, 2006). As such, a second plausible scenario to explain the seasonal progression of sediment trap waxes relative to living plant waxes is that spring (June) waxes at our site were more D-enriched than the late-summer waxes, similar to what Newberry et al. (2015) observed in the UK. This model of seasonal δD_{wax} progression resolves the discrepancy between our leaf and sediment trap samples. That is, waxes entering the lake in mid-summer (July), when δD_{wax} was at a maximum, were likely produced during spring (mid-June), when biosynthetic fractionation is minimal. As the initial waxes were ablated over the weeks following budbreak, they were replaced by more D-depleted waxes, despite increasingly D-enriched xylem waters. δD_{wax} was then relatively stable during our limited sampling window between July and August. This hypothesis is most parsimonious with the relatively D-depleted waxes which enter the lake in late fall and during the spring freshet because the waxes overwintering on land are somewhat depleted relative to the early season waxes and would have been derived from litterfall originating in August and September. We cannot confirm this hypothesis without further sampling May/June leaves. Nonetheless, this point argues for a mixed-season, summer biased precipitation source.

An alternative explanation for the seasonal cycle in sediment trap δD_{wax} is that a subset of plant species on the landscape produce a relatively large quantity of D-enriched waxes during mid-summer, but these waxes do not contribute substantially to the soil/particular leaf matter washed into the lake in spring. If this is the case, our vegetation survey was not broad enough to observe these plant types.

Overall, our observations support the hypothesis that δD of long chain *n*-acids and *n*-alkanes records a summer-biased mean annual precipitation isotope signal in the Arctic. Wilkie et al. (2012) found that the isotopic composition of spring precipitation and streamwater is a good representation of plant source water during the growing season in Siberia. In their study the streamwater isotope values were intermediate between mean annual and summer precipitation values, and the resulting value of ε_{app} was approximately −105‰. We find strong evidence that plants use summer precipitation in the Toolik region, and to a lesser extent, fall and winter precipitation stored in the soil. However, we note that the average composition of plant source waters is similar to $\delta D_{precipitation}$ during spring (May and June). The use of summer precipitation by plants was also observed in Arctic Svalbard, where the δD of plant annual growth rings is more strongly correlated with summer $\delta D_{precipitation}$ than with either winter $\delta D_{precipitation}$ or with the amount of snow accumulation during winter (Blok et al., 2015). These findings have important implications for the interpretation of δD_{wax} records of Arctic paleoclimate, given the potential importance of seasonality in governing high-latitude climate change (Denton et al., 2005).

4.3. Constraining landscape-scale vegetation effects on sedimentary δD_{wax}

Surface sediment δD_{wax} varies by up to 37‰ across our 24 study lakes for a given *n*-acid homologue and by up to 32‰ for a given *n*-alkane homologue. These ranges are substantial, especially if δD_{wax} is to be used for reconstructing paleoclimate – 37‰ is equivalent to ~12 °C of temperature variability based on the modern relationship between temperature and $\delta D_{precipitation}$ of ~3.1‰ °C^{-1} across northern North America (Porter et al., 2016). In the absence of climatic and $\delta D_{precipitation}$ gradients in our constrained study area, we assume that the variability arises principally from local (watershed-scale) variations in vegetation. Quantifying the vegetation effect is therefore important because in Alaska and around the Arctic, deglacial and modern climate warming have been accompanied by vegetation changes, especially an expansion of shrub vegetation (Livingstone, 1955; Tape et al., 2012), which could alter the ecosystem value of ε_{app} and impact reconstructions of past $\delta D_{precipitation}$.

The different glacial landscapes in the Toolik Lake area support diverse and well-characterized vegetation assemblages with varying relative abundances of monocot and eudicot plants over a very small area (Walker et al., 1994), allowing a test of whether catchment-scale differences in vegetation affect δD_{wax} independent of climatic influences. In general, we find that for lakes situated in watersheds with a high abundance of dry and barren tundra, δD_{wax} is 10–30‰ less negative than for those lakes surrounded by sedge and grass-dominated vegetation classes such as moist acidic tundra and wetlands.

Of the nine vegetation classes defined by Walker and Maier (2008), dry tundra and barren/heath tundra are the two classes with the least abundance of monocots. The vegetation in these units predominantly support lichens, dicotyledonous forbs and prostrate shrubs such as *Salix reticulata*. Based on the ε_{app} difference between *E. vaginatum* and *B. nana* in this study and the previously well-described difference between monocots and dicots (Gao et al., 2014a), we expect waxes in lakes surrounded predominantly by dry tundra to be relatively D-enriched. In contrast, wetland areas and moist tundra contain a mix of shrubs, forbs, monocotyledonous graminoids (ex. *Eriophorum* spp. and *Carex* spp.), and *Sphagnum* moss, with graminoids and mosses dominating the biomass (Walker et al., 1994) and so lake sediments in this setting should be relatively D-depleted.

While the vegetation classes are blunt instruments for describing species assemblages, the correlations observed here (Fig. 9, Table A2) are consistent with a vegetation effect. Our study is limited in that we did not track soil and or plant water D/H values from dry tundra ecotypes, and it is possible that differences in δD_{soil} also contributes to the positive relationship of ε_{app} with abundance of dry tundra. Evaporative effects are expected to be small based on our soil water isotope measurements from moist acidic tundra (Fig. 4). However, the extremely shallow organic soils in the dry/barren tundra could result in short soil water residence time, such that δD_{soil} ratios would closely track the seasonal pattern in $\delta D_{precipitation}$, and the contribution of winter precipitation (D-depleted) to soil water is relatively small. Whether δD_{soil} differs across land cover types or not, we suggest that the predominance of eudicots on the dry tundra influences the δD_{wax} we observe in lake sediments via the lower ε_{app} values that characterize eudicot vegetation (Fig. 9).

Watershed scale vegetation effects should be most prominent if waxes are primarily transported through runoff, and least prominent if aeolian transport prevails, as the latter should result in exchange of waxes between watersheds and reduced variability across lakes. While waxes can be transported via wind over long ranges as aerosols (Conte and Weber, 2002; Gao et al., 2014b; Nelson et al., 2017) or particulates (Fahnestock et al., 2000), the large range in sediment δD_{wax} observed among our study lakes suggests that hydraulic transport causes the lake sediment δD_{wax} signal to primarily record watershed scale effects of vegetation and soil. Local transport is further substantiated by the seasonal pattern in wax transport and deposition observed in the lake sediment traps (Fig. 8). Approximately 65% of the total *n*-acids (C_{20}-C_{30}) were deposited between May 16 and July 1, during the spring freshet for Arctic lakes. The most likely explanation for this peak is that waxes are transported by runoff during the period of high snowmelt and mass movement. A predominance of local hydrologic transport contrasts with that of temperate European lakes, where Nelson et al. (2017) find that aeolian transport is most important. The difference could arise because the short stature of Arctic vegetation limits windborne material, or because the snowmelt runoff event is more intense in our study lake catchments than in the European lake catchments. As the summer progresses and snowmelt-derived inputs decline, long-distance aerosol waxes may become more important relative to local hydraulic inputs. Since the late summer wax flux is small, however, watershed scale heterogeneity is preserved in lake sediments.

Overall, the range in the ecosystem scale ε_{app} between lakes is substantially smaller than the potential range based on end-member monocot and eudicot fractionations that we found at the plant scale. The reduced range could be due to some aerosol transport homogenizing the isotope signal between lakes, or simply because within each watershed, plant communities contain a mixture of monocot and eudicot species, and true monocot/dicot end-members are never achieved at the watershed scale. It is evident, based on the scatter in the ε_{app} – vegetation relationship and on the different lipid distributions between *E. vaginatum*, *B. nana*, and the surface sediment waxes, that other plant species contribute a considerable portion of the sedimentary waxes. Thus, while our study species may provide a reasonable representation of two major plant classes, they do not completely capture the variability in δD_{wax} of the contributing tundra plants. In particular, the sedimentary waxes are characterized by dominant chain lengths of C_{27} *n*-alkane and C_{24} *n*-acid, a feature not observed in either study species. A survey of all tundra plant types will help further refine vegetation-based ε_{app} correction methods. Nonetheless, the impact of vegetation assemblages is consistent with expectations based on fractionation among plant types. These data stress the importance of considering independent estimates of paleovegetation, such as pollen (Feakins, 2013) or plant macrofossils (Nichols et al., 2014) when quantitatively determining Arctic $\delta D_{precipitation}$ based on sediment or soil δD_{wax} measurements.

5. CONCLUSIONS

Here we assessed the effects of water uptake, transpiration, biosynthesis, and landscape integration as controls on the D/H fractionation associated with leaf wax formation in Arctic Alaska, and provide estimates of ε_{app} under different vegetation regimes.

We find that ε_{app} values of two of the most abundant plants in the Arctic tundra, *B. nana* and *E. vaginatum*, are similar to shrubs and grasses in non-Arctic sites. This finding is substantiated by direct observations of leaf water isotope enrichment and ε_{app} at the plant-scale as well as ε_{app} at the ecosystem-scale. Likewise, modeled leaf water shows no particularly strong enrichment in a continuous light regime. We propose that the effect of prolonged, 24-h photosynthesis during the Arctic summer on the hydrogen isotopic composition of waxes is small in the low Arctic tundra despite 24-h day lengths.

We take advantage of the strong edaphic control on vegetation assemblages in the Brooks Range foothills to produce the first analysis of a vegetation effect on ε_{app} in the absence of a climatic gradient. Across 24 lakes within 10 km of each other, ε_{app} varied by 44‰. This result suggests that (1) wax transport between watersheds as aerosols is small compared to the hydraulic transport within watersheds and (2) variation in plant assemblages between watersheds plays a significant role in the observed ε_{app}. Using vegetation maps, we demonstrate a positive correlation between the abundance of dry tundra (eudicot-dominant) and ε_{app} for long-chain *n*-acids and *n*-alkanes. The relationship illustrates the necessity of correcting δD_{wax} changes for changes in vegetation, and serves as a guide for such corrections. We propose that for sedimentary records of δD_{wax}, a sliding scale of ε_{app} can be appropriately applied if the relative abundance of eudicots is known.

ACKNOWLEDGEMENTS

Thanks to Alice Carter, Dan White, and William Longo for assistance with field collection. Joe Orchardo, Rafael Tarozo, and Josue Crowther helped with laboratory analyses. This work was partially supported by the ARC LTER (NSF-DEB-1026843), NSF OPP award (1503846), the National Geographic Society, the Brown-MBL joint graduate program, and research grants to Will Daniels from the Geologic Society of American and the Institute at Brown in Environment and Society. The Toolik Lake precipitation isotope data is partially supported by J. Welker's NSF OPP MRI award (0953271) and the Alaska Water Isotope Network (AKWIN).

APPENDIX A. SUPPLEMENTARY MATERIAL

Supplementary data associated with this article can be found, in the online version, at http://dx.doi.org/10.1016/j.gca.2017.06.028.

REFERENCES

Alstad K., Welker J., Williams S. and Trlica M. (1999) Carbon and water relations of Salix monticola in response to winter browsing and changes in surface water hydrology: an isotopic study using δ13C and δ18O. *Oecologia* **120**, 375–385.

Blok D., Weijers S., Welker J. M., Cooper E. J., Michelsen A., Löffler J. and Elberling B. (2015) Deepened winter snow increases stem growth and alters stem δ13C and δ15N in evergreen dwarf shrub Cassiope tetragona in high-arctic Svalbard tundra. *Environ. Res. Lett.* **10**, 044008.

Bowen G. (2015) The Online Isotopes in Precipitation Calculator, version 2.2. <http://www.waterisotopes.org>.

Bowen G. J. and Revenaugh J. (2003) Interpolating the isotopic composition of modern meteoric precipitation. *Water Resour. Res.* **39**, 1299.

Bray E. and Evans E. (1961) Distribution of n-paraffins as a clue to recognition of source beds. *Geochim. Cosmochim. Acta* **22**, 2–15.

CAVM Team (2003) Circumpolar Arctic Vegetation Map. Scale 1:7,500,000. Conservation of Arcic Flora and Fuana (CAFF) Map No. 1. U.S. Fish and Wildlife Service, Anchorage, Alaska.

Chapin, III, F. S., Shaver G. R., Giblin A. E., Nadelhoffer K. J. and Laundre J. A. (1995) Responses of arctic tundra to experimental and observed changes in climate. *Ecology* **76**, 694–711.

Cherry J. E., Déry S. J., Stieglitz M. and Pan F. f. (2014) *Meteorology and Climate of Toolik Lake and the North Slope of Alaska: Past, Present and Future. Alaska's Changing Arctic: Ecological Consequences for Tundra, Streams, and Lakes*. Oxford Univ. Press.

Chikaraishi Y. and Naraoka H. (2007) Δ 13 C and δD relationships among three *n*-alkyl compound classes (*n*-alkanoic acid, *n*-alkane and *n*-alkanol) of terrestrial higher plants. *Org. Geochem.* **38**, 198–215.

Chikaraishi Y., Naraoka H. and Poulson S. R. (2004) Hydrogen and carbon isotopic fractionations of lipid biosynthesis among terrestrial (C3, C4 and CAM) and aquatic plants. *Phytochemistry* **65**, 1369–1381.

Conte M. H. and Weber J. C. (2002) Plant biomarkers in aerosols record isotopic discrimination of terrestrial photosynthesis. *Nature* **417**, 639–641.

Cornwell J. and Kipphut G. (1992) Biogeochemistry of manganese- and iron-rich sediments in Toolik Lake, Alaska. *Hydrobiologia* **240**, 45–59.

Dansgaard W. (1964) Stable isotopes in precipitation. *Tellus* **16**, 436–468.

Denton G., Alley R., Comer G. and Broecker W. (2005) The role of seasonality in abrupt climate change. *Quatern. Sci. Rev.* **24**, 1159–1182.

Drenzek N. J., Montluçon D. B., Yunker M. B., Macdonald R. W. and Eglinton T. I. (2007) Constraints on the origin of sedimentary organic carbon in the Beaufort Sea from coupled molecular 13 C and 14 C measurements. *Mar. Chem.* **103**, 146–162.

Ebbs L. (2016) Response of Arctic shrubs to deeper winter snow is species and ecosystem dependent: an isotopic study in northern alaska. Thesis.

Ehleringer J. and Dawson T. (1992) Water uptake by plants: perspectives from stable isotope composition. *Plant Cell Environ.* **15**, 1073–1082.

Fahnestock J., Povirk K. and Welker J. (2000) Abiotic and biotic effects of increased litter accumulation in arctic tundra. *Ecography* **23**, 623–631.

Feakins S. J. (2013) Pollen-corrected leaf wax D/H reconstructions of northeast African hydrological changes during the late Miocene. *Palaeogeogr. Palaeoclimatol. Palaeoecol.* **374**, 62–71.

Feakins S. J., Warny S. and Lee J.-E. (2012) Hydrologic cycling over Antarctica during the middle Miocene warming. *Nat. Geosci.* **5**, 557–560.

Flanagan L. B. and Ehleringer J. R. (1991) Effects of mild water stress and diurnal changes in temperature and humidity on the stable oxygen and hydrogen isotopic composition of leaf water in *Cornus stolonifera* L.. *Plant Physiol.* **97**, 298–305.

Gao L., Burnier A. and Huang Y. (2012) Quantifying instantaneous regeneration rates of plant leaf waxes using stable hydrogen isotope labeling. *Rapid Commun. Mass Spectrom.* **26**, 115–122.

Gao L., Edwards E. J., Zeng Y. and Huang Y. (2014a) Major evolutionary trends in hydrogen isotope fractionation of vascular plant leaf waxes. *PLoS One* **9**, e112610.

Gao L., Hou J., Toney J., MacDonald D. and Huang Y. (2011) Mathematical modeling of the aquatic macrophyte inputs of mid-chain n-alkyl lipids to lake sediments: implications for interpreting compound specific hydrogen isotopic records. *Geochim. Cosmochim. Acta* **75**, 3781–3791.

Gao L. and Huang Y. (2013) Inverse gradients in leaf wax δD and δ13C values along grass blades of Miscanthus sinensis: implications for leaf wax reproduction and plant physiology. *Oecologia* **172**, 347–357.

Gao L., Zheng M., Fraser M. and Huang Y. (2014b) Comparable hydrogen isotopic fractionation of plant leaf wax n-alkanoic acids in arid and humid subtropical ecosystems. *Geochem. Geophys. Geosyst.* **15**, 361–373.

Garcin Y., Schwab V. F., Gleixner G., Kahmen A., Todou G., Séné O., Onana J.-M., Achoundong G. and Sachse D. (2012) Hydrogen isotope ratios of lacustrine sedimentary *n*-alkanes as proxies of tropical African hydrology: insights from a calibration transect across Cameroon. *Geochim. Cosmochim. Acta* **79**, 106–126.

Gebauer R., Reynolds J. and Tenhunen J. (1998) Diurnal patterns of CO_2 and H_2O exchange of the Arctic sedges *Eriophorum angustifolium* and *E. vaginatum* (Cyperaceae). *Am. J. Bot.* **85**, 592–592.

Hamilton T. D. (2003) Surficial geology of the Dalton Highway (Itkillik-Sagavanirktok rivers) area, southern Arctic foothills, Alaska.

Hou J., D'Andrea W. J. and Huang Y. (2008) Can sedimentary leaf waxes record D/H ratios of continental precipitation? Field, model, and experimental assessments. *Geochim. Cosmochim. Acta* **72**, 3503–3517.

Hou J., D'Andrea W. J., MacDonald D. and Huang Y. (2007) Hydrogen isotopic variability in leaf waxes among terrestrial and aquatic plants around Blood Pond, Massachusetts (USA). *Org. Geochem.* **38**, 977–984.

Huang Y., Shuman B., Wang Y. and Webb T. (2004) Hydrogen isotope ratios of individual lipids in lake sediments as novel tracers of climatic and environmental change: a surface sediment test. *J. Paleolimnol.* **31**, 363–375.

Jasechko S., Lechler A., Pausata F., Fawcett P., Gleeson T., Cendón D., Galewsky J., LeGrande A., Risi C. and Sharp Z. (2015) Glacial–interglacial shifts in global and regional precipitation δ18O. *Clim. Past Discuss.* **11**, 831–872.

Kahmen A., Dawson T. E., Vieth A. and Sachse D. (2011) Leaf wax n-alkane δD values are determined early in the ontogeny of Populus trichocarpa leaves when grown under controlled environmental conditions. *Plant Cell Environ.* **34**, 1639–1651.

Kahmen A., Hoffmann B., Schefuß E., Arndt S. K., Cernusak L. A., West J. B. and Sachse D. (2013a) Leaf water deuterium enrichment shapes leaf wax n-alkane δD values of angiosperm plants II: observational evidence and global implications. *Geochim. Cosmochim. Acta* **111**, 50–63.

Kahmen A., Schefuß E. and Sachse D. (2013b) Leaf water deuterium enrichment shapes leaf wax n-alkane δD values of angiosperm plants I: experimental evidence and mechanistic insights. *Geochim. Cosmochim. Acta* **111**, 39–49.

Klein E., Nolan M., McConnell J., Sigl M., Cherry J., Young J. and Welker J. (2016) McCall Glacier record of Arctic climate change: Interpreting a northern Alaska ice core with regional water isotopes. *Quatern. Sci. Rev.* **131**, 274–284.

Klein E. S., Cherry J. E., Young J., Noone D., Leffler A. J. and Welker J. M. (2015) Arctic cyclone water vapor isotopes support past sea ice retreat recorded in Greenland ice. *Sci. Rep.* **5**, 10295.

Konecky B., Russell J. and Bijaksana S. (2016) Glacial aridity in central Indonesia coeval with intensified monsoon circulation. *Earth Planet. Sci. Lett.* **437**, 15–24.

Leffler A. J. and Welker J. M. (2013) Long-term increases in snow pack elevate leaf N and photosynthesis in Salix arctica: responses to a snow fence experiment in the High Arctic of NW Greenland. *Environ. Res. Lett.* **8**, 025023.

Li C., Sessions A. L., Kinnaman F. S. and Valentine D. L. (2009) Hydrogen-isotopic variability in lipids from Santa Barbara Basin sediments. *Geochim. Cosmochim. Acta* **73**, 4803–4823.

Liu J., Liu W., An Z. and Yang H. (2016) Different hydrogen isotope fractionations during lipid formation in higher plants: implications for paleohydrology reconstruction at a global scale. *Sci. Rep.* **6**, 19711.

Livingstone D. (1955) Some pollen profiles from arctic Alaska. *Ecology*, 587–600.

Longo W. M., Theroux S., Giblin A. E., Zheng Y., Dillon J. T. and Huang Y. (2016) Temperature calibration and phylogenetically distinct distributions for freshwater alkenones: evidence from northern Alaskan lakes. *Geochim. Cosmochim. Acta* **180**, 177–196.

Nelson D. B., Knohl A., Sachse D., Schefuß E. and Kahmen A. (2017) Sources and abundances of leaf waxes in aerosols in central Europe. *Geochim. Cosmochim. Acta* **198**, 299–314.

Newberry S. L., Kahmen A., Dennis P. and Grant A. (2015) N-Alkane biosynthetic hydrogen isotope fractionation is not constant throughout the growing season in the riparian tree Salix viminalis. *Geochim. Cosmochim. Acta* **165**, 75–85.

Nichols J. E., Peteet D. M., Moy C. M., Castañeda I. S., McGeachy A. and Perez M. (2014) Impacts of climate and vegetation change on carbon accumulation in a south-central Alaskan peatland assessed with novel organic geochemical techniques. *The Holocene* **24**, 1146–1155.

Nichols J. E., Walcott M., Bradley R., Pilcher J. and Huang Y. (2009) Quantitative assessment of precipitation seasonality and summer surface wetness using ombrotrophic sediments from an Arctic Norwegian peatland. *Quatern. Res.* **72**, 443–451.

Niedermeyer E. M., Forrest M., Beckmann B., Sessions A. L., Mulch A. and Schefuß E. (2016) The stable hydrogen isotopic composition of sedimentary plant waxes as quantitative proxy for rainfall in the West African Sahel. *Geochim. Cosmochim. Acta* **184**, 55–70.

Oswald W. W., Brubaker L. B., Hu F. S. and Gavin D. G. (2003) Pollen-vegetation calibration for tundra communities in the Arctic Foothills, northern Alaska. *J. Ecol.* **91**, 1022–1033.

Pagani M., Pedentchouk N., Huber M., Sluijs A., Schouten S., Brinkhuis H., Damsté J. S. S. and Dickens G. R. (2006) Arctic hydrology during global warming at the Palaeocene/Eocene thermal maximum. *Nature* **442**, 671–675.

Pautler B. G., Reichart G.-J., Sanborn P. T., Simpson M. J. and Weijers J. W. (2014) Comparison of soil derived tetraether membrane lipid distributions and plant-wax δD compositions for reconstruction of Canadian Arctic temperatures. *Palaeogeogr. Palaeoclimatol. Palaeoecol.* **404**, 78–88.

Polissar P. J. and Freeman K. H. (2010) Effects of aridity and vegetation on plant-wax δD in modern lake sediments. *Geochim. Cosmochim. Acta* **74**, 5785–5797.

Porter T. J., Froese D. G., Feakins S. J., Bindeman I. N., Mahony M. E., Pautler B. G., Reichart G.-J., Sanborn P. T., Simpson M. J. and Weijers J. W. H. (2016) Multiple water isotope proxy reconstruction of extremely low last glacial temperatures in Eastern Beringia (Western Arctic). *Quatern. Sci. Rev.* **137**, 113–125.

Roden J. S. and Ehleringer J. R. (1999) Observations of hydrogen and oxygen isotopes in leaf water confirm the Craig-Gordon model under wide-ranging environmental conditions. *Plant Physiol.* **120**, 1165–1174.

Sachse D., Billault I., Bowen G. J., Chikaraishi Y., Dawson T. E., Feakins S. J., Freeman K. H., Magill C. R., McInerney F. A. and Van der Meer M. T. (2012) Molecular paleohydrology: interpreting the hydrogen-isotopic composition of lipid biomarkers from photosynthesizing organisms. *Annu. Rev. Earth Planet. Sci.* **40**, 221–249.

Sachse D., Gleixner G., Wilkes H. and Kahmen A. (2010) Leaf wax n-alkane δD values of field-grown barley reflect leaf water δD values at the time of leaf formation. *Geochim. Cosmochim. Acta* **74**, 6741–6750.

Sachse D., Radke J. and Gleixner G. (2004) Hydrogen isotope ratios of recent lacustrine sedimentary n-alkanes record modern climate variability. *Geochim. Cosmochim. Acta* **68**, 4877–4889.

Sachse D., Radke J. and Gleixner G. (2006) ΔD values of individual n-alkanes from terrestrial plants along a climatic gradient – implications for the sedimentary biomarker record. *Org. Geochem.* **37**, 469–483.

Sauer P. E., Eglinton T. I., Hayes J. M., Schimmelmann A. and Sessions A. L. (2001) Compound-specific D/H ratios of lipid biomarkers from sediments as a proxy for environmental and climatic conditions. *Geochim. Cosmochim. Acta* **65**, 213–222.

Sessions A. L. (2006) Seasonal changes in D/H fractionation accompanying lipid biosynthesis in Spartina alterniflora. *Geochim. Cosmochim. Acta* **70**, 2153–2162.

Sessions A. L., Burgoyne T. W., Schimmelmann A. and Hayes J. M. (1999) Fractionation of hydrogen isotopes in lipid biosynthesis. *Org. Geochem.* **30**, 1193–1200.

Shanahan T., Hughen K., Ampel L., Sauer P. and Fornace K. (2013) Environmental controls on the 2H1H values of terrestrial leaf waxes in the Eastern Canadian Arctic. *Geochim. Cosmochim. Acta*.

Shaver G. R., Laundre J. A., Bret-Harte M. S., Chapin, III, F. S., Mercado-Díaz J. A., Giblin A. E., Gough L., Gould W. A., Hobbie S. E. and Kling G. W. (2014) *Terrestrial Ecosystems at Toolik Lake, Alaska. Alaska's Changing Arctic: Ecological Consequences for Tundra, Streams and Lakes*. Oxford University Press, New York, pp. 90–142.

Smith F. A. and Freeman K. H. (2006) Influence of physiology and climate on δD of leaf wax *n*-alkanes from C_3 and C_4 grasses. *Geochim. Cosmochim. Acta* **70**, 1172–1187.

Sternberg L. d. S. L. (1988) D/H ratios of environmental water recorded by D/H ratios of plant lipids. *Nature* **333**, 59–61.

Sullivan P. F. and Welker J. M. (2007) Variation in leaf physiology of Salix arctica within and across ecosystems in the High Arctic: test of a dual isotope (Δ13C and Δ18O) conceptual model. *Oecologia* **151**, 372–386.

Tape K. D., Hallinger M., Welker J. M. and Ruess R. W. (2012) Landscape heterogeneity of shrub expansion in Arctic Alaska. *Ecosystems* **15**, 711–724.

Thomas E. K., Briner J. P., Ryan-Henry J. J. and Huang Y. (2016) A major increase in winter snowfall during the middle Holocene on western Greenland caused by reduced sea ice in Baffin Bay and the Labrador Sea. *Geophys. Res. Lett.* **43**, 5302–5308.

Thomas E. K., McGrane S., Briner J. P. and Huang Y. (2012) Leaf wax δ 2 H and varve-thickness climate proxies from proglacial lake sediments, Baffin Island, Arctic Canada. *J. Paleolimnol.*, 1–15.

Tipple B. J., Berke M. A., Hambach B., Roden J. S. and Ehleringer J. R. (2015) Predicting leaf wax n-alkane 2H/1H ratios: controlled water source and humidity experiments with hydroponically grown trees confirm predictions of Craig-Gordon model. *Plant Cell Environ.* **38**, 1035–1047.

Toolik Environmental Data Center Team (2016) *Plant Phenological Monitoring Program at Toolik*. Toolik Field Station, Institute of Arctic Biology, University of Alaska Fairbanks.

Vachon R., Welker J., White J. and Vaughn B. (2010) Monthly precipitation isoscapes (δ18O) of the United States: connections with surface temperatures, moisture source conditions, and air mass trajectories.. *J. Geophys. Res.: Atmos.*, 115.

Walker D. and Walker M. (1996) *Terrain and Vegetation of the Imnavait Creek Watershed, Landscape Function and Disturbance in Arctic Tundra*. Springer, pp. 73–108.

Walker D. A. and Maier H. A. (2008) *Vegetation in the Vicinity of the Toolik Field Station*. University of Alaska. Institute of Arctic Biology.

Walker M. D., Walker D. A. and Auerbach N. A. (1994) Plant communities of a tussock tundra landscape in the Brooks Range Foothills, Alaska. *J. Veg. Sci.* **5**, 843–866.

Ward C. P. and Cory R. M. (2015) Chemical composition of dissolved organic matter draining permafrost soils. *Geochim. Cosmochim. Acta* **167**, 63–79.

Welker J. (2000) Isotopic (δ18O) characteristics of weekly precipitation collected across the USA: an initial analysis with application to water source studies. *Hydrol. Process.* **14**, 1449–1464.

Welker J. M. (2012) ENSO effects on δ18O, δ2H and d-excess values in precipitation across the US using a high-density, long-term network (USNIP). *Rapid Commun. Mass Spectrom.* **26**, 1893–1898.

Welker J. M., Rayback S. and Henry G. H. (2005) Arctic and North Atlantic Oscillation phase changes are recorded in the isotopes (δ18O and δ13C) of Cassiope tetragona plants. *Global Change Biol.* **11**, 997–1002.

White J. W., Cook E. R. and Lawrence J. R. (1985) The DH ratios of sap in trees: Implications for water sources and tree ring DH ratios. *Geochim. Cosmochim. Acta* **49**, 237–246.

Wilkie K., Chapligin B., Meyer H., Burns S., Petsch S. and Brigham-Grette J. (2012) Modern isotope hydrology and controls on δD of plant leaf waxes at Lake El'gygytgyn, NE Russia. *Clim. Past Discuss.* **8**, 3719–3764.

Woo M. k. (2012) *Permafrost Hydrology*. Springer Science & Business Media.

Yang H. and Huang Y. (2003) Preservation of lipid hydrogen isotope ratios in Miocene lacustrine sediments and plant fossils at Clarkia, northern Idaho, USA. *Org. Geochem.* **34**, 413–423.

Yang H., Liu W., Leng Q., Hren M. T. and Pagani M. (2011) Variation in *n*-alkane δD values from terrestrial plants at high latitude: implications for paleoclimate reconstruction. *Org. Geochem.* **42**, 283–288.

Yang H., Pagani M., Briggs D. E., Equiza M., Jagels R., Leng Q. and LePage B. A. (2009) Carbon and hydrogen isotope fractionation under continuous light: implications for paleoenvironmental interpretations of the High Arctic during Paleogene warming. *Oecologia* **160**, 461–470.

Young J., Olga K. and Welker J. M. (2017) Thawing seasonal ground ice: an important water source for boreal forest plants in interior Alaska. *Ecohydrology* **10**. http://dx.doi.org/10.1002/eco.1796.

Associate editor: Alex L. Sessions